Environmental Control on Biotic Development in Siberia (Verkhoyansk Region) and Neighbouring Areas During Permian–Triassic Large Igneous Province Activity

Chapter · July 2020

DOI: 10.1007/978-3-030-47279-5_10

CITATIONS
4

READS
355

6 authors, including:

Yuri D. Zakharov
Russian Academy of Sciences, Far Eastern Branch, Vladivostok
41 PUBLICATIONS **658** CITATIONS
SEE PROFILE

Alexander S. Biakov
Russian Academy of Sciences
100 PUBLICATIONS **1,011** CITATIONS
SEE PROFILE

Micha Horacek
Österreichische Agentur für Gesundheit und Ernährungssicherheit
129 PUBLICATIONS **2,377** CITATIONS
SEE PROFILE

Ruslan Kutygin
Diamond and Precious Metal Geology Institute of the Siberian Branch of the RAS
84 PUBLICATIONS **489** CITATIONS
SEE PROFILE

Jean Guex
John S. Torday
William B. Miller Jr. *Editors*

Morphogenesis, Environmental Stress and Reverse Evolution

Springer

Editors
Jean Guex
Institute of Earth Sciences
Geopolis, UNIL
Lausanne, Switzerland

William B. Miller Jr.
Department of Medicine
Banner Health System
Paradise Valley, AZ, USA

John S. Torday
Department of Pediatrics, Obstetrics
and Gynecology
Evolutionary Medicine Program
David Geffen School of Medicine
University of California
Los Angeles, CA, USA

ISBN 978-3-030-47278-8 ISBN 978-3-030-47279-5 (eBook)
https://doi.org/10.1007/978-3-030-47279-5

This Springer imprint is published by the registered company Springer Nature Switzerland AG
The registered company address is: Gewerbestrasse 11, 6330 Cham, Switzerland

Chapter 10
Environmental Control on Biotic Development in Siberia (Verkhoyansk Region) and Neighbouring Areas During Permian–Triassic Large Igneous Province Activity

Yuri D. Zakharov, Alexander S. Biakov, Micha Horacek, Ruslan V. Kutygin, Evgeny S. Sobolev, and David P. G. Bond

Abstract We propose an updated ammonoid zonation for the Permian–Triassic boundary succession (the lower Nekuchan Formation) in the Verkhoyansk region of Siberia: (1) *Otoceras concavum* zone (uppermost Changhsingian); (2) *Otoceras boreale* zone (lowermost Induan); (3) *Tompophiceras morpheous* zone (lower Induan); and (4) *Wordieoceras decipiens* zone (lower Induan). The *Tompophiceras pascoei* zone, previously defined between the *Otoceras boreale* and *Tompophiceras morpheous* zones, is removed in our scheme. Instead of this the *Tompophiceras pascoei* epibole zone is proposed for the lower part of the *Tompophiceras morpheous* zone. New and previously published nitrogen isotope records are interpreted as responses to climatic fluctuations in the middle to higher palaeolatitudes of

Y. D. Zakharov (✉)
Far Eastern Geological Institute of Russian Academy of Sciences (Far Eastern Branch), Vladivostok, Russia

A. S. Biakov
N.A. Shilo North-East Interdisciplinary Scientific Research Institute, Russian Academy of Sciences (Far Eastern Branch), Magadan, Russia

Kazan (Volga Region) Federal University, Kazan, Russia

M. Horacek
Institute of Lithospheric Research, Vienna University, Vienna, Austria

R. V. Kutygin
Diamond and Precious Metal Geology Institute, Russian Academy of Sciences, Yakutsk, Russia

E. S. Sobolev
Trofimuk Institute of Petroleum Geology and Geophysics, Koptyug Ave. 3, Novosibirsk, Russia

D. P. G. Bond
Department of Geography, Geology and Environment, University of Hull, Hull, UK

J. Guex et al. (eds.), *Morphogenesis, Environmental Stress and Reverse Evolution*, https://doi.org/10.1007/978-3-030-47279-5_10

Northeastern Asia and these suggest a relatively cool climatic regime for the Boreal Superrealm; however the trend towards warming across the Permian–Triassic boundary transition is also seen. The evolutionary development and geographical differentiation of otoceratid ammonoids and associated groups are considered. It is likely that the Boreal Superrealm was their main refugium, where otocerid, dzhulfitid and some other ammonoids survived the major biotic crisis at the end of the Permian. The similarity of ontogenetic development of suture lines of *Otoceras woodwardi* Griesbach and *O. boreale* Spath gives some grounds for suggesting a monophyletic origin of the genus *Otoceras*, having bipolar distribution.

Keywords Permian–Triassic transition · South Verkhoyansk · Molluscs · N-isotopes

10.1 Introduction

The presence of Permian–Triassic (P–T) boundary sequences in Siberia was first documented by Popow (1956, 1958, 1961), who described *Otoceras indigirense* Popow and *O. boreale* Spath from the Indigirka River basin and determined some *Otoceras* from the lower part of the Nekuchan Formation in the South Verkhoyansk region (Setorym River basin) using materials collected by Domokhotov (1960). *Otoceras*-bearing sediments were earlier known only in the Himalayas (Diener 1897) and Greenland (Spath 1930).

The biostratigraphy of the Upper Permian and P–T boundary transition on right bank of the Setorym River, where the Imtachan and Nekuchan formations are well exposed, was initially investigated by Domokhotov (1960) and has since been reported by Korostelev (1972), Arkhipov (1974), Dagys et al. (1984, 1986), and Biakov et al. (2016).

Otoceras boreale Spath from the South Verkhoyansk region was first described by Zakharov (1971) on the basis of his own extensive collection (of more than 150 individual *Otoceras*) from the left bank of the Setorym River. The following biostratigraphic units were recognised from the lower part of the Nekuchan Formation: *Otoceras boreale* beds and overlying "*Vishnuites*" cf. *decipiens* beds (= *Tompophiceras morpheous* zone; Zakharov 2002) on the basis of faunas from the Nikolkin Klyuch and Seryogin Creek sections.

Ammonoids from the *Otoceras*-bearing sequences and overlying units of the Pravyi Suol-1 section have been described by Dagys and Ermakova (1996). Those authors divided the lower part of the Nekuchan Formation into four zones: (1) *Otoceras concavum* (12.0 m thick); (2) *Otoceras boreale* (39.3 m thick); (3) *Tompophiceras pascoei* (13.2 m thick); and (4) *Tompophiceras morpheous* (68.0 m thick) zones. Subsequent investigations (Zakharov 2002; Biakov et al. 2018) suggest that the thicknesses of these units have been significantly overstated by Dagys and Ermakova (1996).

Zakharov (1971, 2002, 2003) has recognised dimorphs in *Otoceras boreale* Spath from the Setorym River basin named "morpha A" (="leaniconchs") and "morpha B" (="faticonchs") (Zakharov 2002). Zakharov (2002) considered these dimorphs to be a strictly corresponding sexual dimorphic pair by analogy with living *Nautilus*. Mature males of living *Nautilus* differ from females in having generally wider (in the apertural region) and larger shells because of presence of the voluminous organ (spadix).

More recently chemostratigraphical (C-isotope) data from P–T boundary sections in the South Verkhoyansk region has been provided by Zakharov et al. (2014, 2015).

In 2016 and 2017, additional expeditions were organised by A.S. Biakov to investigate the bio- and chemostratigraphy of Upper Permian and P–T boundary strata in the Setorym River basin (the Levyi Suol, Pravyi Suol-1, Ustupny and Nikolkin Klyuch sections). The former section has not been investigated previously because until now it was obscured by a debris stream. The latter section has not been visited by geologists during the past 47 years.

This chapter focuses on a revision of data on the stratigraphic distribution of otoceratid and dzhulfitid ammonoids in the P–T boundary strata of the Setorym River basin (South Verkhoyansk region) and the reconstruction of habitats for marine biota existing in the middle and higher palaeolatitudes of Northeast Asia in late Wuchiapingian, Changhsingian and early Induan times based on isotope data. We also evaluate the mass extinction at the end of the Permian and the evolutionary development of otoceratid ammonoids.

Our investigated ammonoid collections are curated at Far Eastern Geological Institute FEB RAN (Vladivostok; collection no. 803) and the Diamond and Precious Metal Geology Institute SB RAN (Yakutsk, collection no. 231).

10.2 Materials and Methods

New macrofossil remains were excavated, prepared and analysed statistically from strata straddling the P–T transition at Pravyi Suol-1, Levyi Suol, Ustupny, Seryogin Creek-2, Nikolkin Klyuch and some other sections in the Setorym River basin (South Verkhoyansk region) for biostratigraphic purposes (Fig. 10.1).

Nitrogen isotope analyses were performed on 144 samples, which were previously analysed for their carbon isotopic composition (Zakharov et al. 2014, 2015). These samples were collected at a spacing of ~0.125–0.14 m in the Imtachan (upper part) and Nekuchan (lower part) formations of the Pravyi Suol-1 section. The samples were ground by a ball mill and decarbonated with 5% HCl on a heated surface. Small aliquots of the samples were weighed into tin capsules and analysed for their N-isotope ratio using a Flash EA (Thermo, Bremen/Germany), connected via a CONFLO IV (Thermo, Bremen/Germany) to a Delta V advantage isotope ratio mass spectrometer (Thermo, Bremen/Germany) in Wieselburg, Austria (HBLFA Francisco–Josephinum). The results are reported in the conventional δ-notation in

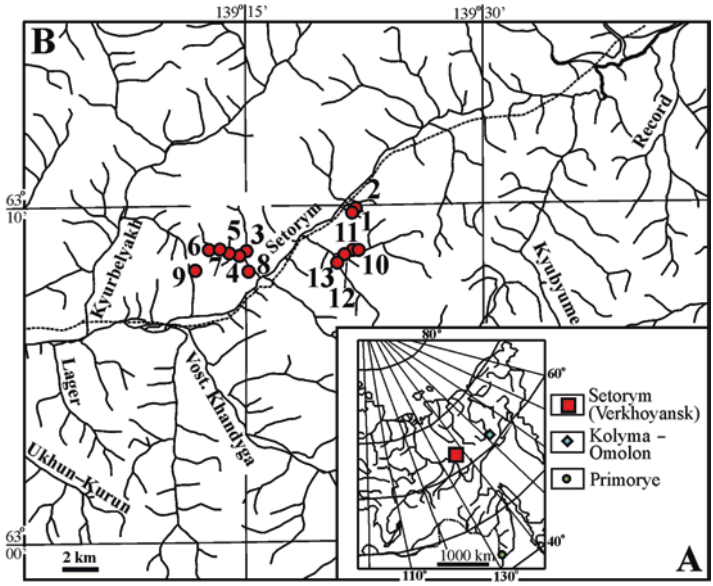

Fig. 10.1 Location map of the investigated area in the Setorym River basin, South Verkhoyansk area. 1, Nikolkin Klyuch (base of section is located at 63°11′56.6″ N, 139°26′35.6″ E); 2, Inessin Klyuch; 3, Levyi Suol (63°08′43.0″ N, 139°14′04.9″ E); 4, Pravyi Suol-1 (63°09′18.5″ N, 139°12′10.9″); 5, Pravyi Suol-2; 6, Pravyi Suol-3; 7, Pravyi Suol-4; 8, Nizhny Suol; 9, Ustupny; 10, Seryogin Creek-1; 11, Seryogin Creek-2; 12, Seryogin Creek-3 (Shagali); 13, Dolgachan

permil (‰) relative to the international N-air standard for nitrogen. Reproducibility of replicate standards is better than ±1‰ for nitrogen (because of the low content of organic matter and corresponding low N content of the samples).

10.3 Results: Biostratigraphy, Nitrogen Isotopes

The studied area (Setorym River basin) is located within the western part of the Verkhoyansk–Kolyma folded area (South Verkhoyansk Zone) adjacent to the eastern edge of the Siberian platform (Parfenov and Kuzmin 2001), where P–T sequences comprise the Imtachan and Nekuchan formations (Domokhotov 1960; Biakov et al. 2016). The upper part of the Imtachan formation (*Intomodesma postevenicum* subzone of the *Intomodesma costatum* zone; Biakov et al. 2016, 2018) in our sections comprises alternations of sandstone, siltstone and sandy siltstone. The exposed part of the overlying Nekuchan Formation in the Pravyi Suol-1 and Levyi Suol sections consists of mudstone (95–100 m thick) with rare layers of sandstone and tuffs.

Following Domokhotov (1960), the P–T boundary was for a long time placed at the Imtachan–Nekuchan formational contact (Zakharov 1971, 1995, 2002; Arkhipov 1974; Korostelev 1972; Dagys et al. 1984, 1986; Dagys and Ermakova 1996). However, chemostratigraphical (C-isotope) data across the P–T boundary transition

at the Pravyi Suol-1 section (Zakharov et al. 2014, 2015; Biakov et al. 2018) have demonstrated that the P–T boundary in the South Verkhoyansk region is located within the *Otoceras*-bearing sequences in the lower part of the Nekuchan Formation. In the Pravyi Suol-1 and Levyi Suol sections, the P–T boundary is placed at approximately 6.3 m above the formational contact (Zakharov et al. 2014, 2015).

The following ammonoid zones are recognised in the lower part of the Nekuchan Formation (from oldest to youngest), modified from Domokhotov (1960), Zakharov (1971, 2002), Dagys et al. (1979, 1984, 1986), Dagys and Ermakova (1996), Zakharov et al. (2014) and Biakov et al. (2018): (1) *Otoceras concavum*, (2) *Otoceras boreale*, (3) *Tompophiceras morpheous* and (4) *Wordieoceras decipiens*. The *Tompophiceras pascoei* zone, offered by Dagys and Ermakova (1996), has been rejected by us, because the first representatives of its species–index were collected from the *Otoceras boreale* zone and their later representatives occur in association with *Tompophiceras morpheous* (Popow) in the Nikolkin Klyuch and Seryogin Creek sections, which are characterised by the most abundant mollusc fossils in the region. However, following epibole zones are offered additionally for the lower and upper parts of the *Tompophiceras morpheous* zone in the Nikolkin Klyuch section: *Tompophiceras pascoei* and *Tompophiceras morpheous*, respectively. On the right bank of the Setorym River (e.g. Levyi Suol, Pravyi Suol-1 and Ustupny), representatives of the genus *Tompophiceras* were reliably found only within members 7–9, corresponding to the *Tompophiceras morpheous* zone.

Additional palaeontological data from the P–T boundary beds in our investigated sections from the Setorym River basin are given below.

10.3.1 Nikolkin Klyuch

The Nikolkin Klyuch section (Fig. 10.2) is located on the left bank of the Setorym River, ~19 km upstream from its mouth. This section is accessible by car, as it is only 0.6 km SE of the road, but it is located on a very steep slope in the ravine. Nikolkin Klyuch is one of the most complete P–T boundary sections in Siberia, containing members 1–11 of the Imtachan (upper part) and Nekuchan (lower part) formations (see lithological column in Fig. 10.3). Otoceratid, dzhulfitid and some other ammonoids described by Zakharov (1971, 2002, 2003) are from this section. The recent revision of some ammonoid species from this section and the additional collection of fossil material in 2016 permit clarification and revision of the fauna.

No fossils were found in the upper part of member 1 of the Imtachan formation or in member 2 of the Nekuchan Formation represented by sandstone; otoceratid ammonoids in submember 3a of member 3 of the Nekuchan Formation (4.2 m thick), belonging to the *Otoceras concavum* zone, are quite rare. Samples collected on the left slope of the Nikolkin Klyuch ravine, 1.0 m above the base of member 3, contain *Otoceras* cf. *gracile* Tozer (Fig. 10.4d–h; Plate 10.1 (1, 2)). Some specimens of this species, found in the member 3a (= member 26; Zakharov et al. 2014), were previously erroneously determined as *Otoceras boreale* Spath (morpha A; Zakharov 2002).

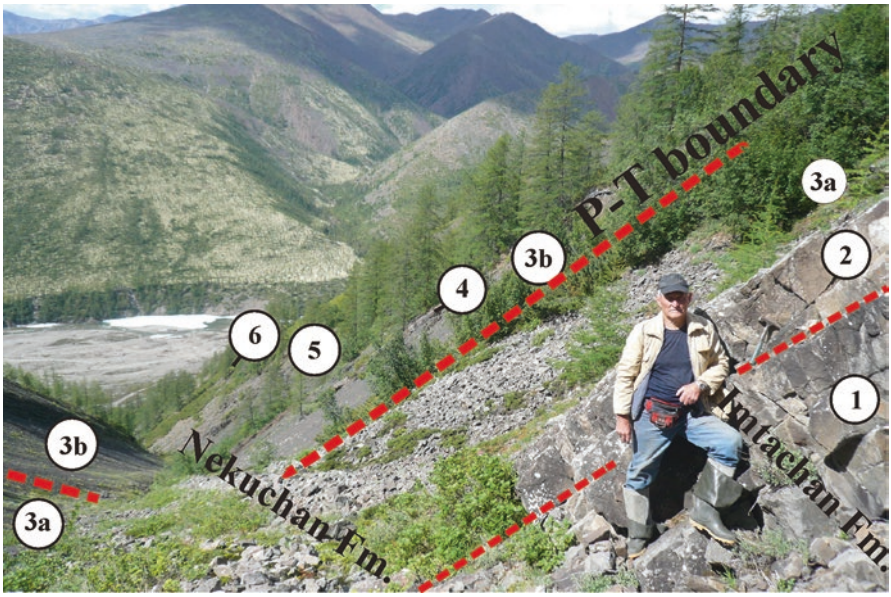

Fig. 10.2 Outcrop photograph showing the location of different units in the Imtachan (uppermost part) and Nekuchan formations (Nikolkin Klyuch section)

Three samples of the *Otoceras concavum* Tozer were found in submember 3a (left slope of the ravine), ~4.0 m above the base of member 3 and from talus (Fig. 10.4a, b; Plates 10.1 (3, 4) and 10.2 (1)). Some specimens of this species, found in the submember 3a (=26; Zakharov et al. 2014), were also previously erroneously determined as *Otoceras boreale* Spath (morpha B; Zakharov 2002).

Submember 3b of member 3, corresponding to the lower part of the *Otoceras boreale* zone, is characterised by both the *O. boreale* morpha A and *O. boreale* morpha B (Figs. 10.4j–n; Plates 10.1 (5) and 10.2 (2)). These are associated with other ammonoid species (e.g. *Aldanoceras* sp.), the nautiloid *Tomponautilus setorymi* Sobolev, the bivalve *Claraia?* sp. and small gastropods and conodonts.

The most abundant collection *Otoceras boreale* originates from 0.3 m-thick layer, situated ~5.2 m above the base of member 3. The conodonts *Hindeoodus typicalis* (Sweet) and *Clarkina* cf. *changhsingensis* Wang et Wang and the earliest representative of the genus *Tompophiceras* (*T.* cf. *pascoei* (Spath)) were discovered in this layer. This 0.3 m-thick layer, which dates to the lower part of the *Otoceras boreale* zone, is proposed as the epibole zone of the same name. A large specimen of *Otoceras boreale* morpha B (Plates 10.2 (5) and 10.2 (2)) was found slightly higher in the sequence, 0.5 m below the top of the member 3.

No fossils have been found in the sandstone belonging to member 4. In overlying mudstone of the lower–middle part of member 5 mollusc remains are extremely rare in the section (only *O. boreale* morpha A has been found somewhat below its top). However, rare ammonoids belonging to *Tompophiceras pacoei* (Spath), *T. morpheous* (Popow) and *Aldanoceras* sp. as well as the bivalve *Claraia?* sp. are common in its upper part, 2–3 m below its top.

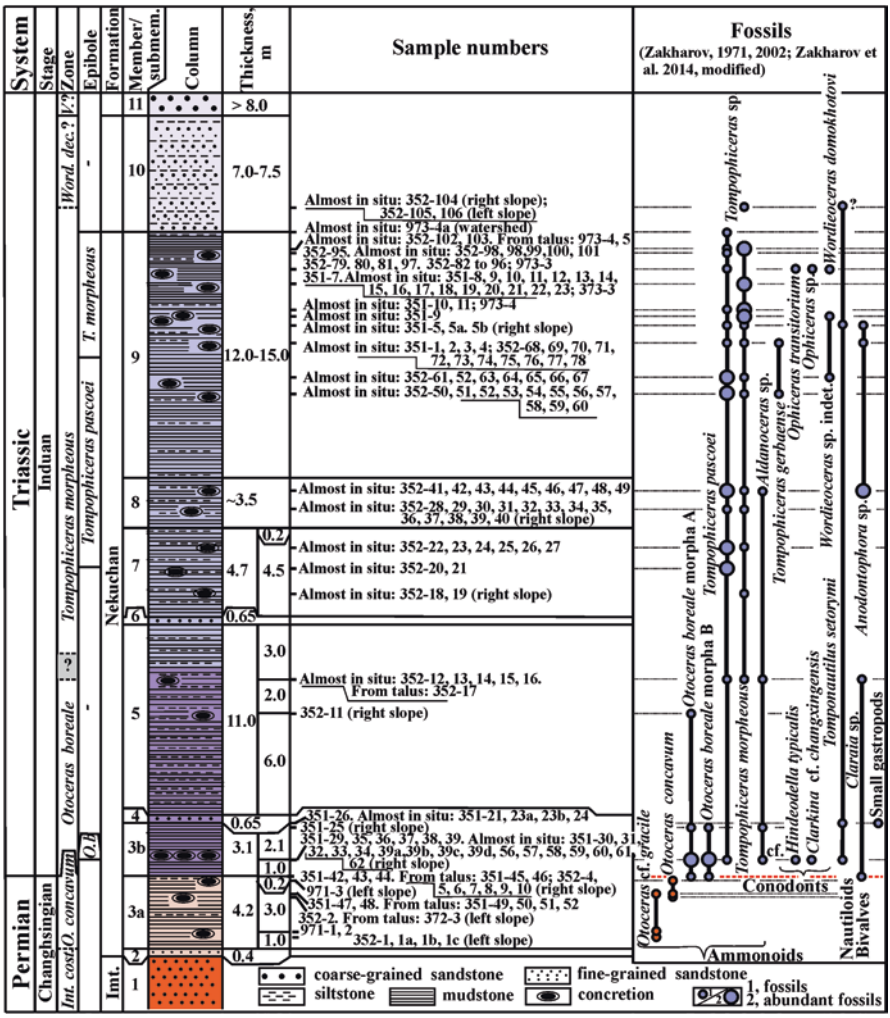

Fig. 10.3 Stratigraphic range chart of important fossils from Permian–Triassic transition of the Nikolkin Klyuch section. Abbreviations: *Int. cost.* Intomodesma costatum, *O. concavum Otoceras concavum*, *Word. dec.*? *Wordieoceras decipiens*, *V.? Vavilovites sverdrupi*, *O.b. Otoceras boreale* epibole-zone, *Imt* Imtachan, *submem.* submember

No fossils have been found in the sandstone of member 6. Members 7 (upper part), 8 and 9 (lower part) represent a *Tompophiceras pascoei* epibole zone, belonging to the *Tompophiceras morpheous* zone, and are rich in individuals of the ammonoid *Tompophiceras pascoei*, as well as *Tompophiceras morpheous*, *Aldanoceras* sp., *Wordieoceras* sp. indet. and some other fossils.

The upper part of member 9, representing a *Tompophiceras morpheous* epibole zone as a part of the zone of the same name, is rich in *Tompophiceras morpheous*, associated with rarer representatives of *T. pascoei* (Spath), *Wordieoceras domokhotovi* Zakharov, the nautiloid *Tomponautilus setorymi* Sobolev and some other fossils.

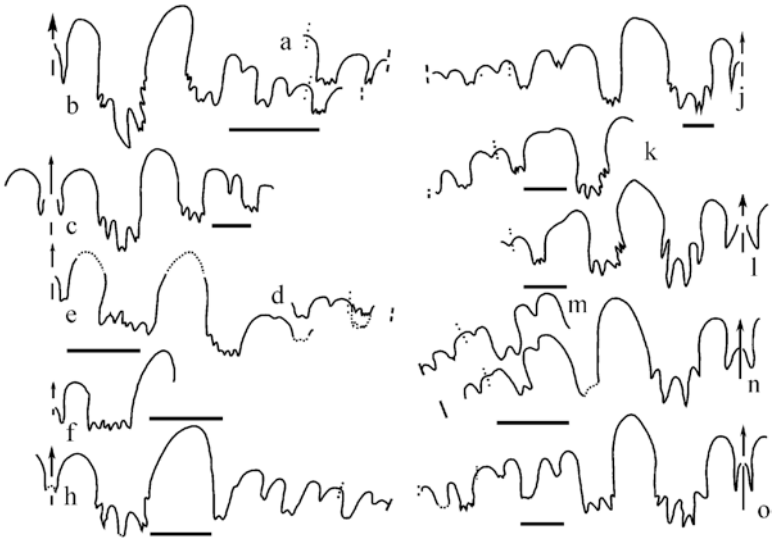

Fig. 10.4 Suture lines of *Otoceras* from the Setorym River basin (a, b), *O. concavum*, FEGI no. 93/803 (field no. 971-30), Nikolkin Klyuch: (a) at $H = 25.5$ mm; (b) at $H = 25.0$ mm; (c) *O. concavum*, DPMGI no. 234/241-1, Ustupny, at $H = 48.0$ mm; (d–h) *O.* cf. *gracile*, Nikolkin Klyuch: (d) FEGI no. 91/803 (field no. 971-2), at $H = 42.5$ mm; (e) FEGI no. 91/803 (field no. 971-2), at $H = 42.3$ mm; (f) FEGI no. 91/803 (field no. 971-2); at $H = 23.9$ mm; (h) FEGI no. 90/803 (field no. 971-1), at $H = 42.2$ mm; (j, l), *O. boreale* morpha B, Nikolkin Klyuch: (j) FEGI no. 31/802 (field no. 351-25), at $H = 76.5$ mm; (k) FEGI no. 80/803 (field no. 351-59), at $H = 56.0$ mm; (l) FEGI no. 80/803 (field no. 351-59), at $H = 51.0$ mm; (m–o) *O. boreale* morpha A: (m) FEGI no. 3/803 (field no. 351-59), at $H = 35.5$ mm, Nikolkin Klyuch; (n) same sample, $H = 35.2$ mm; (o) FEGI no. 151/803 (field no. 970-1), at $H = 58.1$ mm, Levyi Suol. Scale bar 5 mm

The lower part of member 10 is characterised by very rare fossils (e.g. *Tompophiceras* sp.). No fossils were discovered in overlying deposits in this section (lower–middle part of member 10), corresponding apparently to the *Wordioceras decipiens* zone, known for the Lekeer Creek area, Tompo River basin (Dagys and Ermakova 1996).

10.3.2 Inessin Klyuch

The Inessin Klyuch section, located in a neighbouring ravine, 0.4 km upstream from the Nikolkin Klyuch section, is similarly exposed and has comparable member thicknesses. Limited time was spent collecting fossils from this newly discovered section. Therefore, only *Otoceras boreale* Spath was discovered in the upper part of member 3, corresponding to the lower part of the *Otoceras boreale* zone (R.V. Kutygin's coll.). *Tompophiceras pascoei*, collected from the uppermost part of member 9, cor-

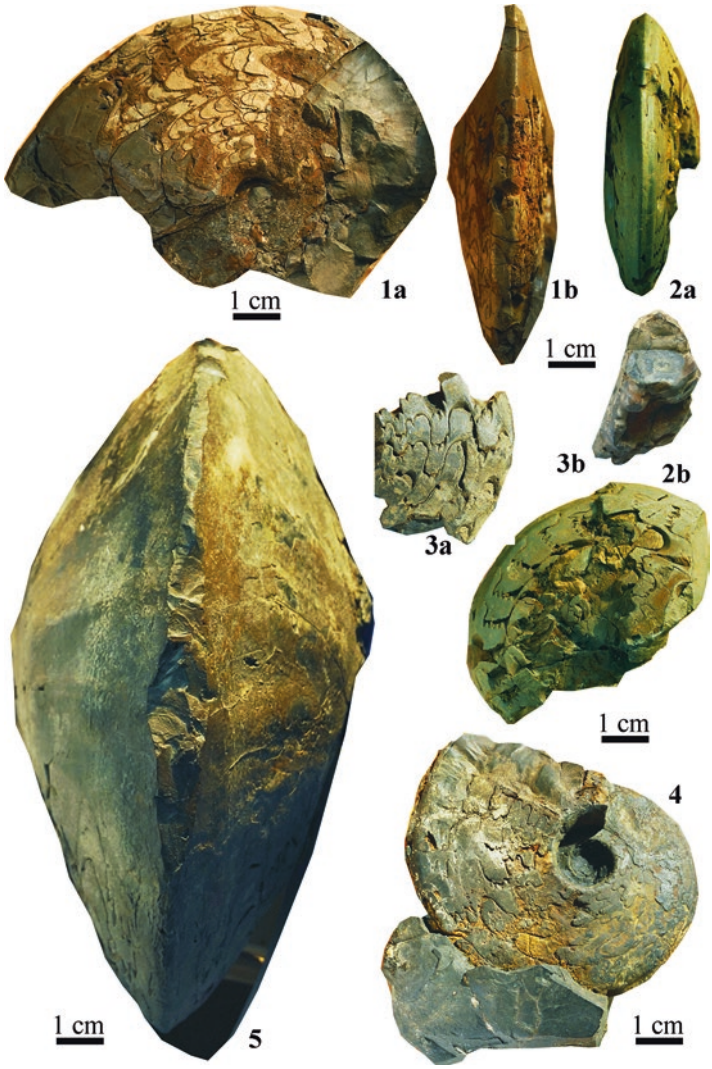

Plate 10.1 (1, 2) *Otoceras* cf. *gracile* Tozer: (1) FEGI no. 90/803 (field no. 971-1); (2) DVGI no. 91/803 (field. no. 971-2); Nikolkin Klyuch; Nekuchan Formation, submember 3a, *Otoceras concavum* zone. (3, 4) *O. concavum* Tozer: (3) FEGI no. 92/803 (field no. 351–49); (4) 93/803 (field no. 971-3); Nikolkin Klyuch; Nekuchan Formation, submember 3a, *Otoceras concavum* zone; (5) *Otoceras boreale* Spath, morpha B, FEGI no. 31/803 (field no. 351-25); Nikolkin Klyuch; Nekuchan Formation, member 3b, *Otoceras boreale* zone

Plate 10.2 (1) *Otoceras concavum* Tozer, FEGI no. 93/803 (field no. 971-3); Nikolkin Klyuch; Nekuchan Formation, submember 3a, *Otoceras concavum* zone. (2) *Otoceras boreale* Spath, morpha B, FEGI no. 31/803 (field no. 351-25); Nikolkin Klyuch; Nekuchan Formation, submember 3b, *Otoceras boreale* zone

responding to the *Tompophiceras morpheous* zone, has been discovered at the Nikolkin Klyuch–Inessin Klyuch watershed (A.M. Popov's coll.).

10.3.3 Levyi Suol and Pravyi Suol-1

The mouth of the Suol Creek is located on the right bank of the Setorym River, 6 km upstream from the mouth of the latter. There are six studied sections recording the P–T boundary transition in the Suol Creek basin: Levyi Suol, Pravyi Suol-1, Pravyi

Suol-2, Pravyi Suol-3 and Nizhny Suol (Fig. 10.1). The most complete and representative sections are Levyi Suol and Pravyi Suol-1 sections.

The Levyi Suol section, recently exposed by a powerful storm event, is located 0.2 km upstream from the Levyi Suol–Pravyi Suol confluence. Pravyi Suol-1 is located just 100 m west of the Levyi Suol section, and so it might be reasonable to consider these as a single section (Fig. 10.5). The Pravyi Suol-1 and possibly Nizhny Suol sections were earlier examined during the excursion organised within the framework of the 27th International Geological Congress in 1984 (Dagys et al. 1984). The majority of the ammonoids described by Dagys and Ermakova (1996) are from the Pravyi Suol-1 section. The Levyi Suol section is undoubtedly the better

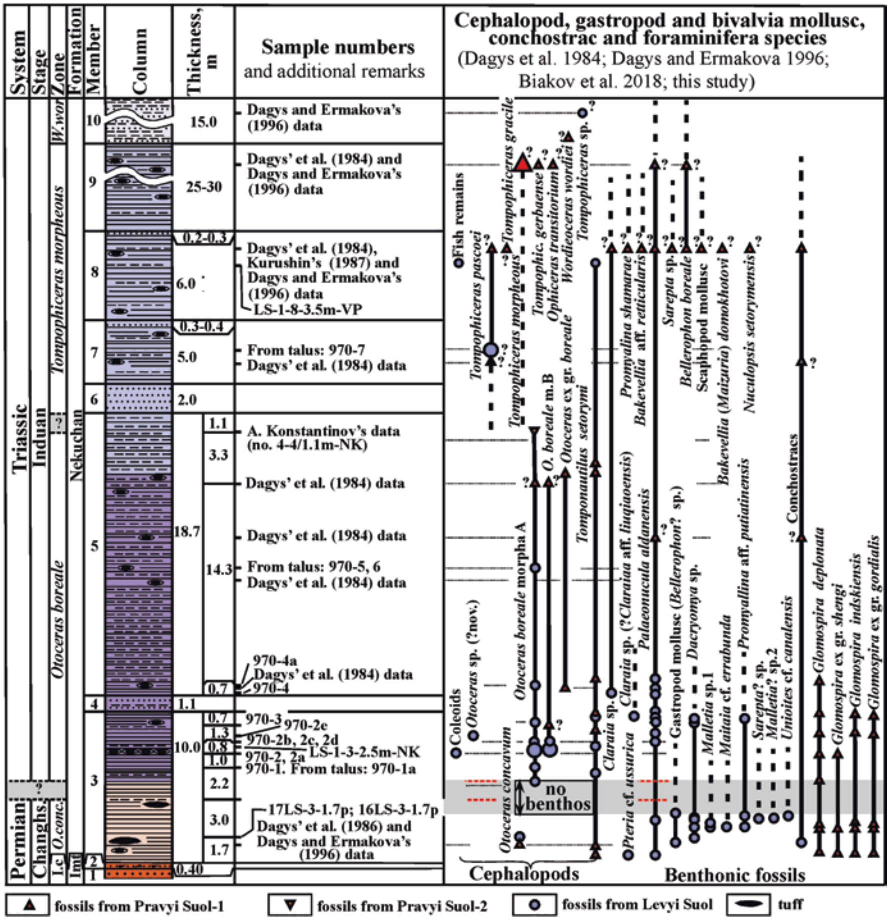

Fig. 10.5 Stratigraphic range chart of important guide fossils from Permian–Triassic transition of the Levyi Suol section. Abbreviations: *Changhs.* Changhsingian, *I.c. Intomodesma costatum*, *O. conc. Otoceras concavum*, *W.dec. Wordieoceras decipiens*. Dashed lines (black and red) show the interval of the possible position of the P-T boundary

exposed of these now, but it was not suitable for detailed research at the time of this earlier excursion.

Attention is drawn to the fact that the lithologic members of the Nekuchan Formation produced in these sections attain a slightly larger thickness than the corresponding members at Nikolkin Klyuch. The lithological description of Pravyi Suol-1 and the stratigraphical distribution of its mollusc and foraminifera fossils, as well as its C-isotope values, have been previously published (Dagys et al. 1984; Kurushin 1987; Dagys and Ermakova 1996; Zakharov et al. 2014, 2015; Biakov et al. 2018).

Member 1 (*Intomodesma postevenicum* subzone of the *Intomodesma costatum* zone) of the Imtachan formation, represented mainly by sandstone, is better exposed in the Pravyi Suol-1 section, 20 m below its top. Sandstone of this subzone yields latest remains of the characteristic typical high-boreal fauna, strongly dominated by *Inoceramus*-like bivalves: *Intomodesma postevenicum* Biakov, *Intomodesma* sp. and *Maitaia* sp. (Biakov et al. 2016, 2018). No fossils have been found in the uppermost 20 m part of member 1, nor in 0.4 m thick member 2 (the basal layer of the Nekuchan Formation represented by sandstone yielding numerous argillite intraclasts).

The lower part of member 3 at Pravyi Suol-1 yields individuals *Otoceras concavum* Tozer (Dagys and Ermakova 1996) which are associated with *Tomponautilus setorymi* Sobolev (Sobolev 1989). Representatives of *Otoceras concavum* were found 1.2 m above the base of member 3 (Dagys et al. 1986). Benthonic foraminifera were collected 0.6 m above the base of member 3, and these were determined by A.V. Yadrenkin as *Ammodiscus septentrionalis* Gerke, *Glomospira deplanata* Kasatkina, *G. indskiensis* Kasatkina and *G.* ex gr. *shengi* Ho (Biakov et al. 2018).

In the Levyi Suol section, two *Otoceras concavum* shells have been collected from the following level of member 3: 1.7 m above its base (Plate 10.3 (2); R.V. Kutygin, E.S. Sobolev and I.L. Vedernikov's coll.). In the lower part of member 3, corresponding apparently to the lower part of the *Otoceras concavum* zone, the following rare bivalves were discovered in association with gastropods and conchostracans: *Palaeonucula aldanensis* Kurushin, *Dacryomya* sp. (dominant), *Malletia?* sp., *Sarepta?* sp., *Myalina* aff. *putiatinensis* (Kiparisova), *Pteria* cf. *ussurica* (Kiparisova), *Maitaia* cf. *errabunda* (Popow) and *Unionites* cf. *canalensis* (Catullo) (Biakov et al. 2018).

No benthic fossils were found at Levyi Suol in the interval from 2.8 to 5.5 m above the base of member 3, which apparently corresponds to the upper part of the *Otoceras concavum* zone. This largely coincides with the interval characterised by a very pronounced manifestation of authigenic pyrite (Biakov et al. 2018).

The upper part of member 3 at Levyi Suol, in interval from 5.7 to 10 m above its base, is characterised by *Otoceras boreale* Spath (Fig. 10.4o; Plate 10.3 (3, 4); A.N. Kilyasov, R.A. Kutygin, E.S. Sobolev and Y.D. Zakharov's coll.). This interval undoubtedly correlates with the lower part of the *Otoceras boreale* zone. The most abundant *Otoceras boreale* specimens, represented by both morpha A and morpha B, are found 7.2 m above the base of member 3. A shell fragment of a possible new *Otoceras* species, characterised by an unusually wide umbilicus, was discovered at

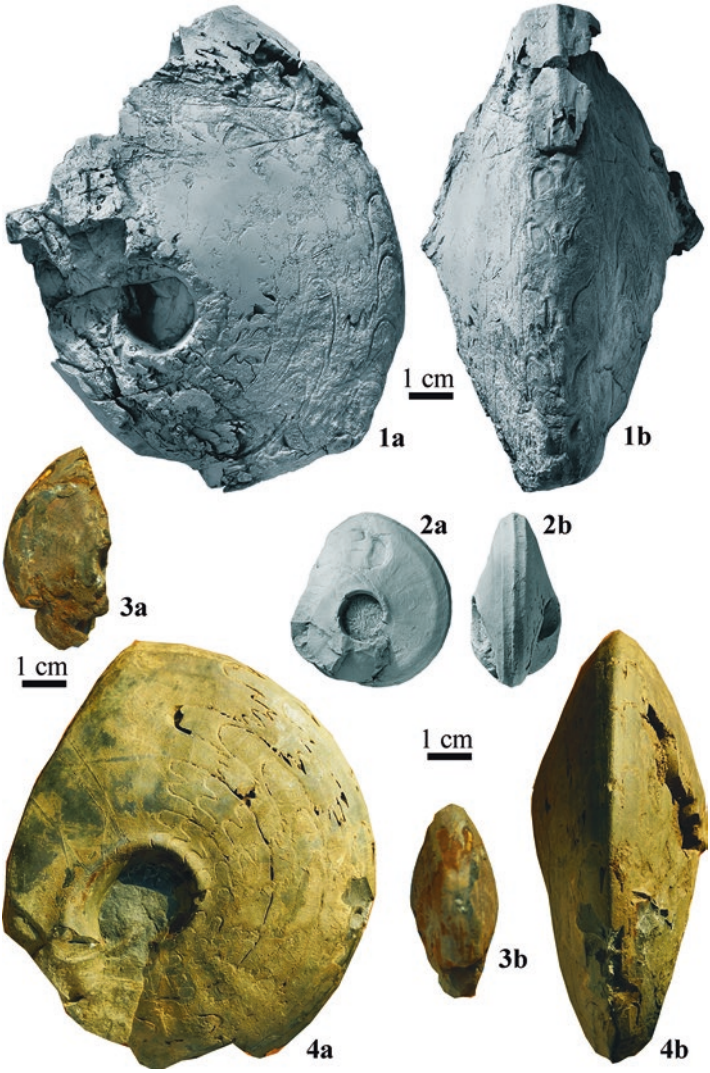

Plate 10.3 (1, 2) *Otoceras concavum* Tozer: (1) DPMGI no. 234/241-1 (field no. 17R1-711.1p); Ustupny; Nekuchan Formation, member 3 (lower part), *Otoceras concavum* zone; (2) DPMGI no. 234/209 (field no. 17LS-3-1.7p+); Levyi Suol; Nekuchan Formation, member 3 (lower part), *Otoceras concavum* zone; (3, 4) *Otoceras boreale* Spath, morpha A: (3) FEGI no. 108/803 (field no. 970-1a); Levyi Suol; Nekuchan Formation, member 3 (upper part), *Otoceras boreale* zone; (4) FEGI no. 105/803 (field no. 970-1); Levyi Suol; Nekuchan Formation, member 3 (upper part), *Otoceras boreale* zone

8.3 m above the base of member 3. The upper part of the member 3 is characterised by the following bivalve species: *Palaeonucula aldanensis* Kurushin (dominant), *Dacryomya* sp., *Myalina* aff. *putiatinensis* (Kiparisova) and ?*Claraia* aff. *linqiaoensis* (He et al.) (Biakov et al. 2018), *Tomponautilus setorymi* Sobolev and more rare coleoids (phragmocone fragment) occur also from this level. In the neighbouring Pravyi Suol-1 section this interval is characterised by the following benthonic fossils: foraminifera *Ammodiscus septentrionalis* Gerke, *Glomospira deplanata* Kasatkina, *G. indskiensis* Kasatkina, *G.* ex gr. *shengi* Ho and *Glomospira* ex gr. *gardialis* (Jones et Parker) (A.V. Yadrenkin's determination; Suol-1 section, Setorym River basin, South Verkhoyansk Biakov et al. 2018) and bivalves *Palaeonucula aldanensis* Kurushin and *Myalina* aff. *putiatinensis* (Kiparisova) (Kurushin 1987). Rare *Otoceras boreale* was collected 0.2 m above the base of member 5 (Y.D. Zakharov's coll.) in the middle part of member 5 (shell fragments; A.M. Popov's coll.) and its upper part. Other fossils, collected in the lower part of the member 5 in the Pravyi Suol-1 section, are represented by bivalves *Palaeonucula aldanensis* Kurushin and *Claraia* sp. and nautiloid *Tomponautilus setorymi* Sobolev, in the Levyi Suol section foraminifera *Ammodiscus septentrionalis* Gerke (Biakov et al. 2018). Member 8 in Levyi Suol yields nautiloid *Tomponautilus setorymi*, associated with fish remains (Sobolev 1989). A few *Tompophiceras pascoei* shells were found in upper members of the Levyi Suol section, but many other *Tompophiceras* from members 8 and 9 of the Pravyi Suol-1 section were described by Dagys and Ermakova (1996). Representatives of *Wordieoceras decipiens* (Spath) have been found in many sections in the *Wordieoceras decipiens* zone, overlaying the *Tompophiceras morpheous* zone (Dagys and Ermakova 1996). However, their stratigraphical position in the Pravyi Suol-1 section has not been strictly determined by these taxa. *Otoceras*-bearing sequences have also been discovered in other sections in the Suol Creek basin (Fig. 10.1).

10.3.4 Ustupny

This is the most complete section of the Upper Permian Imtachan Formation in the South Verkhoyansk region (Domokhotov 1960; Biakov et al. 2016). According to R.V. Kutygin's data, the overlying Nekuchan Formation is also exposed in the watershed part of this section. The lower part of the Ustupny section is similar to the sequences at Pravyi Suol-1 and Levyi Suol. Ammonoid *Otoceras concavum* Tozer (Fig. 10.4c, Plate 10.3 (1); R.V. Kutygin and A.N. Kilyasov's coll.) and nautiloid *Tomponautilus setorymi* Sobolev were found 1.1 m above the base of member 3 of the Nekuchan Formation. *Otoceras boreale* was found at the top of this member, also in association with *Tomponautilus setorymi*. The upper part of the section is characterised by ammonoids of the genus *Tompophiceras*.

10.3.5 Seryogin Creek-1 and -2

The lower part of the member 3 of the Nekuchan Formation, apparently corresponding to the upper Changhsingian *Otoceras concavum* zone, has been identified in locality 339 (Seryogin Creek-1), ca 840 m up from the mouth of Seryogin Creek (Figs. 10.1 and 10.6B). They lie above the dark, poorly sorted fine-grained sandstones that comprise the basal bed (member 2) of the Nekuchan Formation.

The upper part of member 3, which belong to the lower part of the *Otoceras boreale* zone, is exposed at locality 338 (Seryogin Creek-2; Zakharov 1971), situated in the upper part of the southern hillside ca 600 m up from the mouth of Seryogin Creek (Figs. 10.1 and 10.6A). This member is composed of mudstone with numerous calcareous-siliceous concretions that contain *Otoceras boreale* morpha A and *O. boreale* morpha B. Despite the fact that most of the fossils collected from this section were not found in situ, the position of the slope leads us to suggest that the first representatives of *Tompophiceras pascoei* occur from this section in the upper part of member 3, corresponding to the lower part of the *Otoceras boreale* zone. The upper members of the section, composed mainly of mudstone and siltstone, are characterised by *Tompophiceras morpheous* and *Aldanoceras* sp. However, member 10 (interbedding medium-grained and banded fine-grained sandstones), exposed in the lower part of the slope, is conventionally assigned to the *Wordieoceras decipiens* zone.

10.3.6 Seryogin Creek-3 (Shagali) and Dolgachan

In the Seryogin Creek-3 (Shagali) section, situated 460 m up from the mouth of Seryogin Creek, R.V. Kutygin documented the Imtachan/Nekuchan formational contact and found *Otoceras concavum* 2 m above the base of member 3.

Otoceras-bearing deposits of the Dolgachan section, located along the Dolgachan Creek, 720 m up from the mouth of Seryogin Creek, are poorly exposed. *Tompophiceras* was collected by R.V. Kutygin only in the Dolgachan–Seryogin (Shagali) confluence.

10.3.7 Nitrogen Isotopes

Our isotope results, obtained from the Pravyi Suol-1 section are shown in Fig. 10.7. The minimum $\delta^{15}N$ values within the selected N-isotope intervals ("a"–"e") are −0.9‰, and the maximum values do not exceed +3‰ (Zakharov et al. in press); $\delta^{13}C_{org}$ values fluctuate between −30.3 and −26.3‰ (Zakharov et al. 2014, 2015).

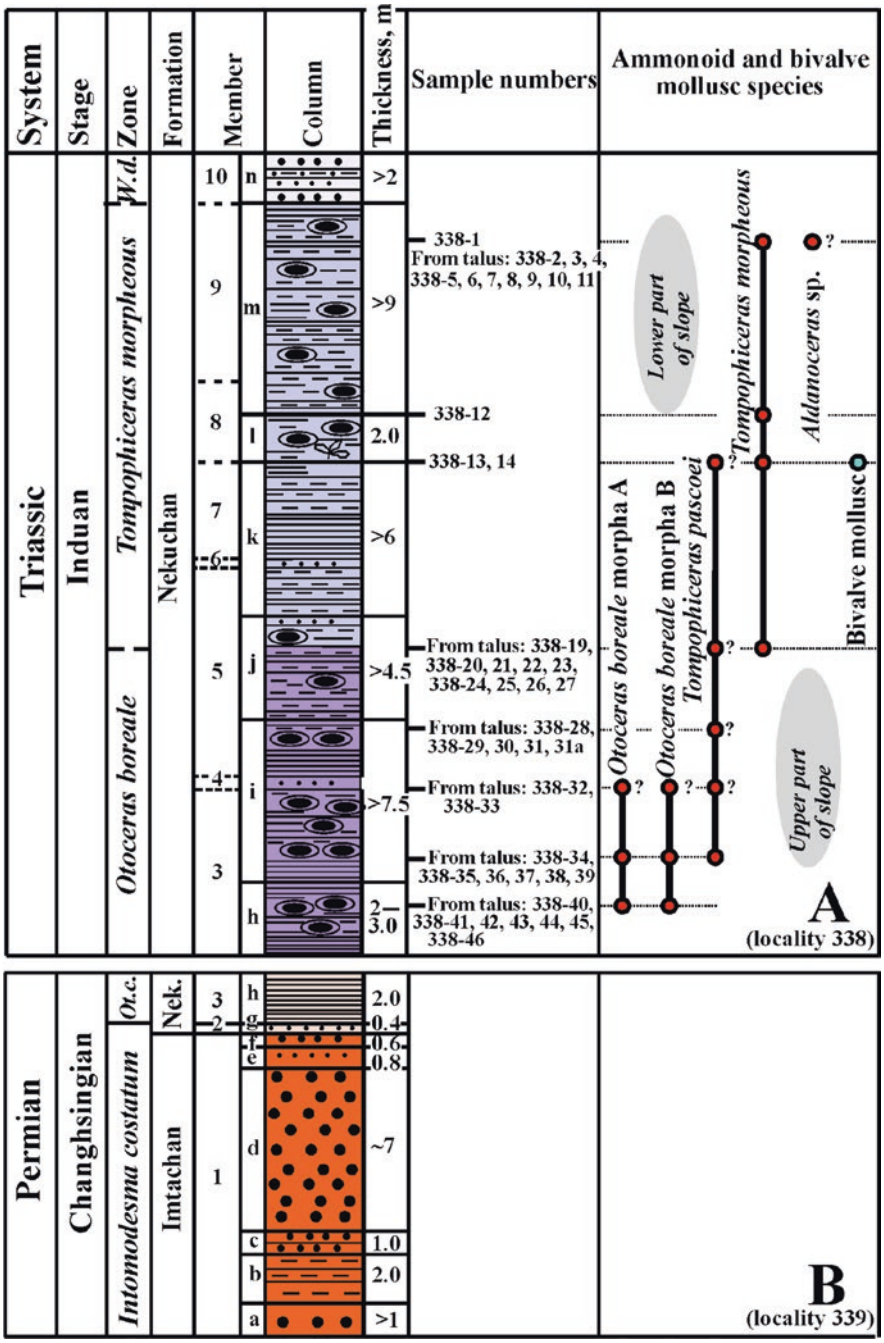

Fig. 10.6 Stratigraphic range chart of important guide fossils from Permian–Triassic transition of the Seryogin Creek-1 and -2 sections. (**B**) Seryogin Creek-1; (**A**) Seryogin Creek-2. Abbreviations: *Ot.c. Otoceras concavum*, *W.d. Wordieoceras decipiens*, Nek. Nekuchan

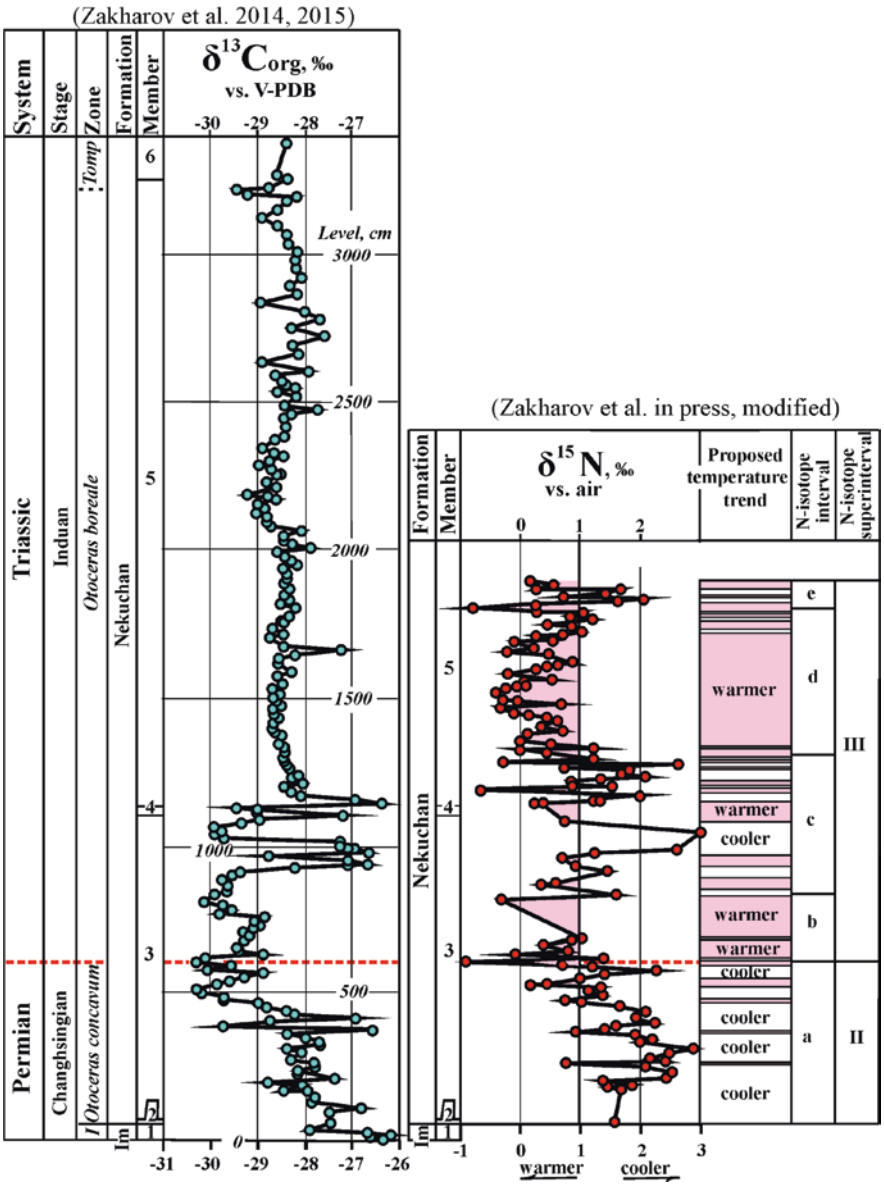

Fig. 10.7 N- and C-isotope composition of Changhsingian and Induan deposits of the Pravyi Suol-1 section, Setorym River basin, South Verkhoyansk area. Abbreviations: *I. Intomodesma costatum*, *Tomp. Tompophiceras morpheous*, Im Imtachan

10.4 Discussion

10.4.1 Reconstruction of Environmental Conditions Influencing Biotic Development in the Middle to High Palaeolatitudes of Eastern Russia During the Late Permian and Early Triassic

It is widely considered that the mass extinction at the end of the Permian was the greatest biotic crisis of the Phanerozoic (fewer than half of the latest Permian marine families survive into the Triassic; Yin and Song 2013). However, the causes of this extinction are still debated.

Of the many triggers proposed for end-Permian extinction, several feature prominently in multiple extinction scenarios: (1) lethally hot temperatures during the latest Permian and into Early Triassic greenhouse (e.g. Knoll et al. 2007; Sun et al. 2012; Goudemand et al. 2013; Romano et al. 2013; Schobben et al. 2014; Grigoryan et al. 2015); (2) anoxia in the oceans (e.g. Wignall and Hallam 1992; Wignall and Twitchet 1996, 2002; Isozaki 1997; Twitchet et al. 2001; Kato et al. 2002; Biakov and Vedernikov 2007; Horacek et al. 2007b; Bond and Wignall 2010; Korte and Kozur 2010; Dustira et al. 2013); (3) catastrophic release of seafloor methane (e.g. Krull et al. 2000; Kaiho et al. 2001, 2009); (4) loading of toxic metals (e.g. Hg) and sulphide to the oceans (e.g. Knoll et al. 2007; Hammer et al. 2019); (5) denudation of terrestrial matter after mass extinction of terrestrial plants and devastation of forests (e.g. Grasby et al. 2013, 2018), possibly linked to ozone damage and increased ultraviolet (UV-B) radiation (Cockell et al. 2000); and (6) bolide/comet impact (e.g., Kaiho et al. 2001, 2009; Lozovsky 2013). Of these, 1–5 have their origins in Siberian flood basalt volcanism (e.g. Hermann et al. 2010; Korte and Kozur 2010), which is widely acknowledged as the ultimate driver of this crisis.

We hope that the following discussion will be a useful contribution to the debate around the end-Permian mass extinction in marine settings in low and higher palaeolatitudes.

Various isotope data provide important constraints for environmental and palaeoclimatic reconstructions. The $^{13}C_{org}$ and $^{13}C_{carb}$ records of Upper Permian and Lower Triassic strata are well known in many regions (e.g. Baud et al. 1989; Wignall et al. 2015; Kaiho et al. 2001, 2009; Horacek et al. 2007a, b, c, 2009; Algeo et al. 2008, 2014; Grasby and Beauchamp 2008; Nakrem et al. 2008; Hermann et al. 2010, 2011; Korte and Kozur 2010; Takashi et al. 2010, 2013; Luo et al. 2011; Song et al. 2013; Zakharov et al. 2014). In Korte and Kozur's (2010) opinion, the Permo–Triassic negative C-isotope excursions, including the major negative $\delta^{13}C$ shift seen globally at the end of the Permian, most likely had their origin in (1) direct and indirect effects of the Siberian Traps and contemporaneous volcanism and (2) the effects of anoxic deepwaters occasionally reaching very shallow marine settings. Short-term events, such as the release of isotopically light methane from the ocean, are questionable as causes for the C-isotope excursions (Korte and Kozur 2010). However, some data, including geochemical (Ce/Ce^*) results, argue against global

anoxia as a cause for the end-Permian mass extinction (Krull et al. 2000; Kozur 2007; Garbelli et al. 2014).

Despite much progress globally, the O- and N-isotope records for the Upper Permian and the Lower Triassic are still poorly known for many regions, including in Siberia and the Russian Far East. Oxygen isotope values, calculating useful proxy for Late Permian and Early Triassic palaeotemperatures, have so far been calculated from the following few materials: (1) calcite of Wuchiapingian and Changhsingian brachiopods from the Caucasus (Zakharov et al. 1999, 2005), Iran (Schobben et al. 2014) and the Kolyma–Omolon region (Zakharov et al. 2005); (2) apatite of Wuchiapingian and Changhsingian conodonts from South China (Sun et al. 2012; Goudemand et al. 2013; Romano et al. 2013), Iran (Schobben et al. 2014) and Transcaucasia (Grigoryan et al. 2015); and (3) aragonite of Olenekian cephalopods from Arctic Siberia (Zakharov et al. 1975, 1999).

$^{15}N_{org}$ records from the Upper Permian and Lower Triassic are restricted to data from South China (e.g. Luo et al. 2011; Jia et al. 2012; Yin et al. 2012; Algeo et al. 2014; Saitoh et al. 2014), Arctic Canada (Algeo et al. 2012; Knies et al. 2013; Grasby et al. 2015, 2016) and the South Primorye (Zakharov et al. 2018a, b, c) and Kolyma–Omolon (Zakharov et al. 2019) regions of Russia. Other recently published isotope data include sulphur isotope profiles from the P–T boundary transition in Japan and Australia (e.g. Horacek et al. 2010; Takashi et al. 2013).

Stable O-isotope analyses of Late Permian and Early Triassic well-preserved conodont and brachiopod fossils from palaeoequatorial regions and adjacent areas suggest water palaeotemperatures of 20–38 °C (Zakharov et al. 1999, 2005; Schobben et al. 2014; Grigoryan et al. 2015; Joachimsky et al., 2012, 2020) and 28–40 °C and higher (Sun et al. 2012; Goudemand et al. 2013; Romano et al. 2013), respectively. However, there is some difficulty in explaining the low $\delta^{18}O$ values in well-preserved aragonite cephalopod shells from the Boreal Superrealm (Arctic Siberia), which also suggest very high water temperatures assuming that they retained normal salinity (Zakharov et al. 1975, 1999).

Nitrogen is a key nutrient necessary for the existence of living organisms. It is a major component of biomass and is required for photosynthesis (Robinson et al. 2012). The majority of the molecular nitrogen is fixed from air by certain types of cyanobacteria (Bauersachs et al. 2009). As a result, ammonium compounds (NH_4+) and ammonia (NH_3) are usually formed. These products are well assimilated by plants, which in turn are used as food resources by animals.

Of greater interest in the light of our research are data on the N-isotopic composition of marine sediments deposited in both greenhouse and icehouse conditions (e.g. Altabet et al. 1995; Jenkyns et al. 2001; Algeo et al. 2008, 2014). Algeo et al. (2014) indicated that Neoproterozoic and Phanerozoic greenhouse climate modes were characterised by low $\delta^{15}N_{sed}$ values (fluctuating from ~−2 to +2‰), whereas icehouse climate modes showed higher $\delta^{15}N$ values (ranging from ~+4 to +8‰; Fig. 10.8a). A general trend of higher $\delta^{15}N_{sed}$ values during times of cool climate and low $\delta^{15}N_{sed}$values during warm periods is explained apparently by several processes, including (1) the increased microbiological denitrification in cooler conditions, when nitrates (NO_3^-) are reduced to nitrite (NO_2^-) and further to nitrogen gas (N_2)

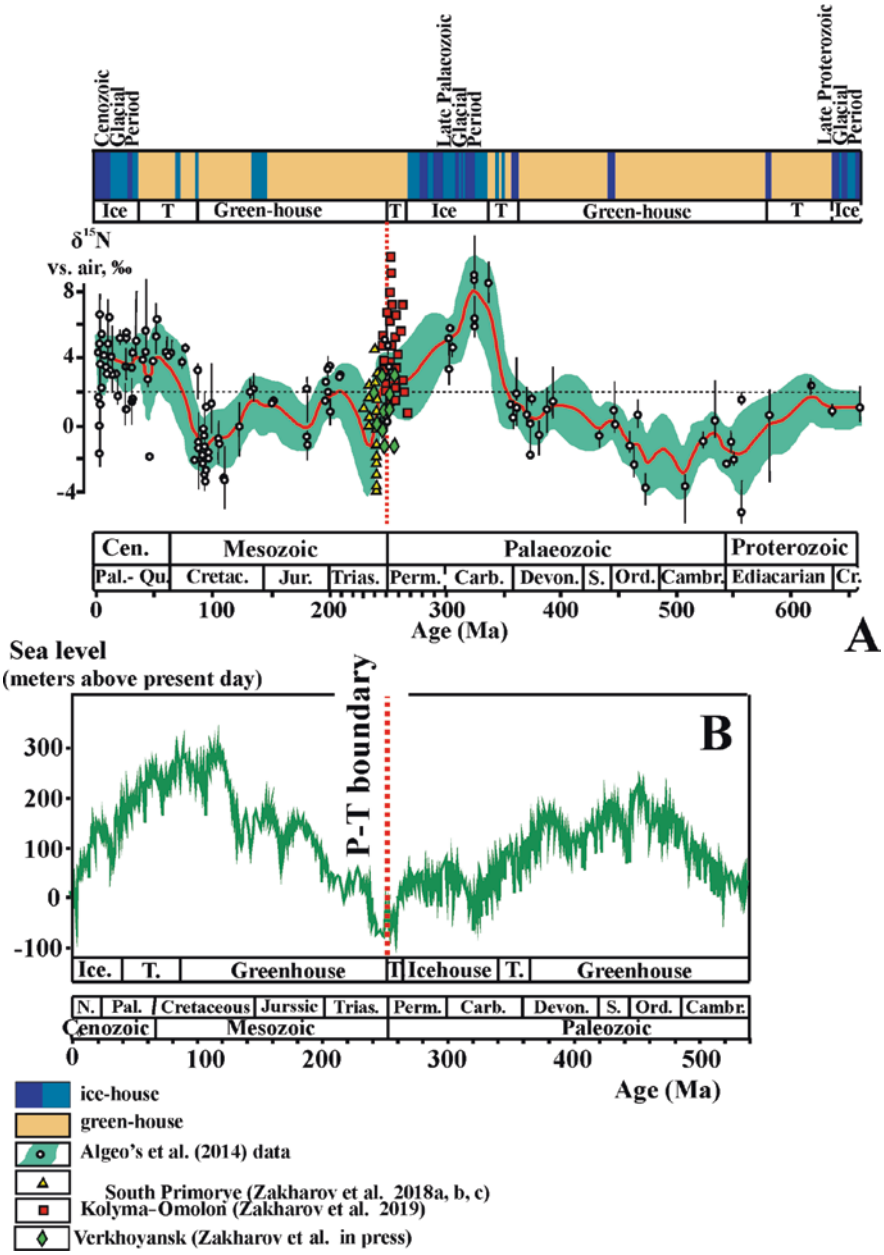

Fig. 10.8 (**a**) Long-term secular variation in marine sediment $\delta^{15}N$ values, based on study units of Proterozoic–Cenozoic age (Algeo et al. 2014) with an addition (this study); (**b**) data on sea-level fluctuation (Boulila et al. 2018). Abbreviations: *Ice* Ice house, *T* Transition, *Pal.–Qu.* Palaeogene–Quaternary, *Cretac.* Cretaceous, *Jur.* Jurassic, *Trias.* Triassic, *Carb.* Carboniferous, *Devon.* Devonian, *S.* Silurian, *Ord.* Ordovician, *Cambr.* Cambrian, *Cr.* Cryogenian

which is returned to the atmosphere, and (2) the increased nitrogen fixation from the air, realised by cyanobacteria in warmer conditions (Luo et al. 2011; Algeo et al. 2014).

The general correlation between δ^{18}O-palaeotemperature and δ^{15}N curves, as shown for the Kamenushka-1, Kamenushka-2, Pautovaya and Pravyi Suol-1 sections (Zakharov et al. 2018a, b, 2019), supports the idea described in Zakharov et al. (2018c) that intervals with high δ^{15}N values in the P–T sections of Russia mainly reflect the presence of lower temperature conditions in comparison with intervals with low δ^{15}N values. This interpretation stimulates our attempts to distinguish both N-isotope superintervals in Permian and Triassic of the eastern part of Russia, as well as their subdivisions (N-isotope intervals), which may indicate climatic and particular temperature variations (Fig. 10.9). An example of the first of these are

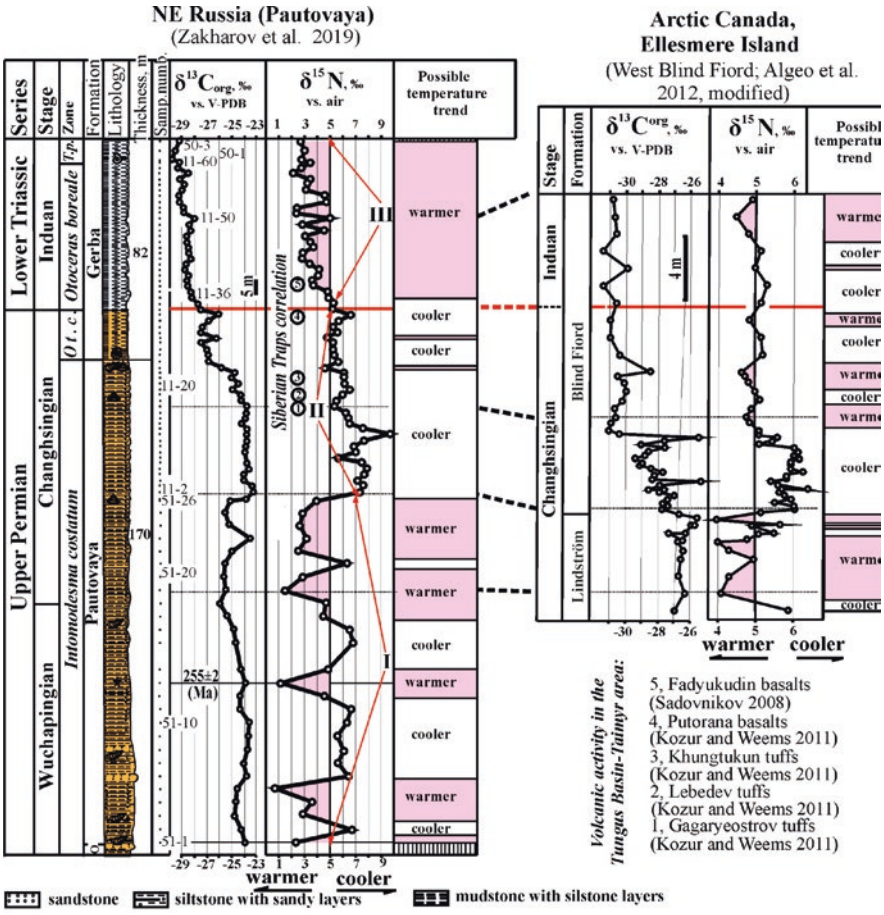

Fig. 10.9 Correlation of C- and N-isotope records from the Permian–Triassic Pautovaya section (Kolyma–Omolon region) with composite record from West Blind Fiord (Arctic Canada). Abbreviations: *Ot.c. Otoceras concavum*, *T. Tompophiceras*, *O* Ovod

N-isotope superintervals I–IX, distinguished in the Wuchiapingian, Changhsingian and Induan of the northern regions of eastern Russia and in the Lower and Middle Triassic of the southern regions (Zakharov et al. 2018a, b, c, 2019). An example of the shorter ones (N-isotope intervals) is "a"–"e", recognised in the P–T boundary transition in the South Verkhoyansk region (Zakharov et al. in press). However, in this discussion we are going to concentrate our attention only on N-isotope superintervals I–III (Fig. 10.9) and on N-isotope intervals "a"–"e" (Fig. 10.7).

By interpreting the N-isotope data to be at least in part a function of temperature, our results from the Kolyma−Omolon region suggest oscillating but generally warm temperature conditions prevailed in the late Wuchiapingian and early Changhsingian (N-isotope superinterval I; Fig. 10.9), as well as in the Sverdrup Basin, Arctic Canada (Algeo et al. 2012). In the middle Changhsingian rather cooler conditions developed (apparently just before the first volcanic activity in the Siberian Traps) before a gradual shift towards warmer and less variable climatic conditions in the late Changhsingian (the upper part of the N-isotope superinterval II; Fig. 10.9). The contemporaneous Gagaryeostrov, Lebedev and Khungtukan tuff accumulations (Kozur and Weems 2011) in northern Siberia might have driven some of this warming trend but apparently did not cause major climatic and environmental instability. This interpretation is supported by the stable development of gymnosperms at the same time in what is now Norway (Hermann et al. 2010; Hochuli et al. 2010) as well as the high taxonomic biodiversity of Siberian flora (Sadovnikov 2008, 2016). A similar climatic development apparently occurred in the Sverdrup Basin, Canada, according to the similarity of the N-isotope data from Pautovaya (Zakharov et al. 2019) and West Blind Fiord (Algeo et al. 2012). A further shift towards warmer and generally quite consistent conditions in Northeast Russia (Kolyma–Omolon and South Verkhoyansk regions) and Arctic Canada is inferred for the earliest Induan (N-isotope superinterval III; Fig. 10.9).

N-isotope data for the Pravyi Suol-1 section (N-isotope intervals "a"–"e", located within the superintervals II (upper part) and III; Fig. 10.7) provide a detailed record of proposed temperature changes in the P–T transition in the Boreal Superrealm. A steady shift towards warmer temperatures beginning near the end of the Changhsigian (N-isotope interval "a", corresponding to the *Otoceras concavum* zone) was followed by markedly warmer conditions at the beginning of the Induan (N-isotope interval "b", corresponding to the lowest part of the *Otoceras boreale* zone). The subsequent N-isotope interval "c", corresponding to the lower part of the same *Otoceras boreale* zone (the upper part of member 3, member 4 and the lower part of member 5) might have been characterised by the frequent alternation of relatively cooler and warmer conditions. This interval is followed by the N-isotope interval "d", characterised by warmer conditions (*Otoceras boreale* zone—the middle part of member 5). The N-isotope data of the following brief interval, known from the middle part of member 5 (N-isotope interval "e"), corresponding to the middle part of the same *Otoceras boreale* zone, seems to once again be characterised by frequent alternations between relatively cooler and warmer conditions.

It is worth noting that comparisons of N-isotope data with data on eustatic sea-level fluctuations in the Phanerozoic time (Fig. 10.8a, b) (e.g. Algeo et al. 2014; Boulila

et al. 2018) show a good agreement, this serving as additional evidence for temperature being the dominant driver of both N-isotope variations and sea-level fluctuations..

As mentioned above, previous studies support extreme warmth in equatorial and southern moderate palaeolatitudes for some periods during the Early Triassic (e.g. Schobben et al. 2014). However, the absence of $\delta^{15}N$ values below −0.9‰ in the P–T sections of the Boreal Superrealm (e.g. Verkhoyansk, Kolyma–Omolon and Arctic Canada; Algeo et al. 2012; Zakharov et al. 2019; this study—Fig. 10.8a) in contrast to sections from more southernly palaeolatitudes of Russia (South Primorye—Abrek, Kamenushka-1 and Kamenushka-2; Zakharov et al. 2018a, b) might be explained by the clearly cooler environments of deposition of the former locations at higher palaeolatitudes.

The warming at the very end of the Changhsingian and the beginning of the Induan could have been caused by the latest Changhsingian Putorana basalt event, which occurred during the main phase of Siberian Traps eruptions. It is assumed (e.g. Kozur and Weems 2011) that this activity injected large volumes of greenhouse gases, including CO_2 and CH_4 to the atmosphere, resulting in the Late Permian mass extinction which is documented in many regions of the Tethys (e.g. Baud et al. 1989; Kaiho et al. 2009. This event has been correlated with marked changes in environment in Norway: there is an evidence of extinction of one of the large groups of gymnosperms (Glossopteridales; Hermann et al. 2010) at the P–T boundary there.

Algeo et al. (2012) recognised two P−T marine environmental and biotic crises in Arctic Canada. The contact between the chert of the Lindström formation and the silty shale of the overlying Blind Fiord formation in the Sverdrup Basin records, in their opinion, a regional extinction of siliceous sponges (first Arctic extinction event; Algeo et al. 2012). In the South Verkhoyansk region this event is linked with the disappearance of typical high-boreal fauna (*Inoceramus*-like bivalves), latest remains of which were found 20 m below the top of the Upper Permian Imtachan formation (Biakov et al. 2018).

The second P−T crisis in Arctic Canada is associated with intensified anoxia and a possible change in phytoplankton community composition (Algeo et al. 2012). In South Verkhoyansk, the interval of 2.8–5.5 m above the base of the uppermost Changhsingian–Induan Nekuchan Formation in the Levyi Suol and Pravyi Suol-1 sections is characterised by no benthonic fossils, which were seen in adjacent intervals (Biakov et al. 2018), and the pronounced manifestation of authigenic pyrite, potentially indicating anoxic or euxinic conditions, by analogy with P−T boundary sections in Svalbard (Bond and Wignall 2010). We suggest that this interval corresponds to the second episode of the marine environmental and biotic crisis in Arctic Canada (Algeo et al. 2012) and latest Permian mass extinction event, documented in Tethyan shallow-marine sections (e.g. Yin and Zhang 1996; Burgess et al. 2014; Brosse et al. 2016). In contrast to the first episode of the Late Permian marine environmental crises, the second phase in the Verkhoyansk region did not cause major biotic changes (e.g. Biakov et al. 2018). This assumption, made mainly on the basis of data on benthonic fossils (bivalve molluscs and foraminifera), is consistent with the data on semi-pelagic fossils—ammonoids of the genus *Otoceras* and nautiloid of the species *Tomponautilus setorymi* Sobolev.

10.4.2 The Evolutionary Development and Geographical Differentiation of Otoceratid and Dzhulfitid Ammonoids

Only the following five known ammonoid succession lineages at different levels survived the end-Permian mass extinction (Fig. 10.10): (1) *Paratirolites–Tompophiceras* (at the family level—Dzhulfitidae; Arkhipov 1974; Zakharov and Moussavi Abnavi 2013; Zakharov and Popov 2014); (2) *Hypophiceras triviale* (Spath)–*Hypophiceras martini* (Spath) (at the generic level—*Hypophiceras*; Bjerager et al. 2006); (3) *Otoceras concavum* Tozer–*Otoceras boreale* Spath (at the generic level—*Otoceras*; this study); (4) *Episageceras wynnei* (Waagen)–*Episageceras antiquum* (Popov) (at the generic level—*Episageceras*; Popow 1961; Zakharov 1978; Dagys and Ermakova 1996; Zakharov and Moussavi Abnavi 2013; Zakharov and Popov 2014); and (5) *Episageceras wynnei* (Waagen)–*Episageceras dalailamae* (Diener) (at the generic level—*Episageceras*; Diener 1897). It is notable that all these, with the exception of *Episageceras*, survived into the Triassic within the Boreal Superrealm.

Data relating to the genus *Tompophiceras* (Popow 1961) obtained from northeast Russia (Nikolkin Klyuch and Seryogin Creek sections, South Verkhoyansk region) provide some evidence that its first representatives were coexisting with the earliest Induan *Otoceras boreale* Spath (this study).

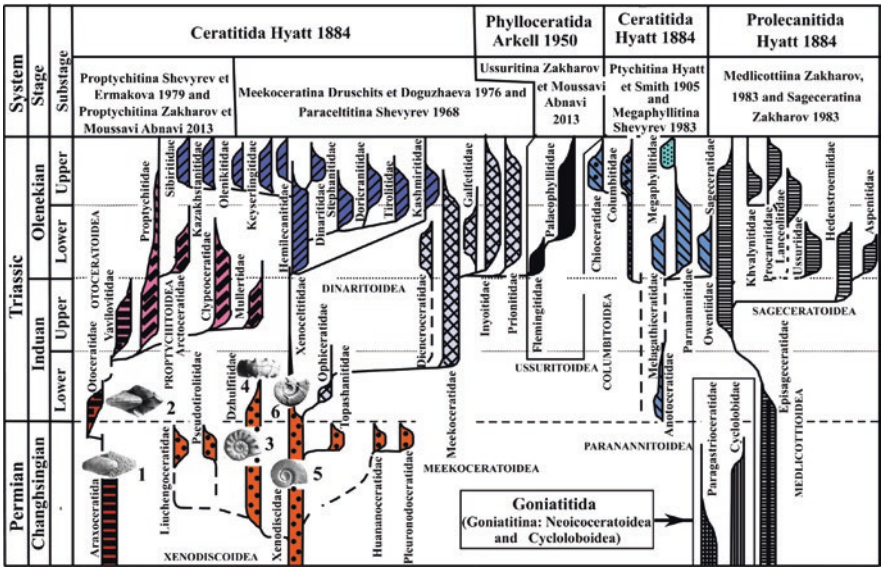

Fig. 10.10 Phylogenetic relationships of the Permian–Triassic goniatitid, prolecanitid, ceratitid and phylloceratid ammonoid superfamilies and families (modified from Zakharov and Moussavi Abnavi 2013). 1, *Avushoceras*; 2, *Otoceras*; 3, *Paratirolites*; 4, *Tompophiceras*; 5, *Xenodiscus*; 6, *Aldanoceras*

Early Induan ammonoids of the genus *Episageceras*, described by Noetling (1904) on the basis of data on the species "*Sageceras*" *wynneri* Waagen from the Upper Permian in the Salt Range, are known in the Boreal Superrealm as *Episageceras antiquum* (Popow) (after Dagys and Ermakova's (1996) revision). *Episageceras* shells were collected by different authors from Kobyume (South Verkhoyansk, *Otoceras boreale* zone; Popow 1961), Burgagandzha (South Verkhoyansk, *Vavilovites turgidus* and *Kingites korostelevi* zones; Zakharov 1978; Dagys and Ermakova 1996) and Okhotsk sea-coast region (*Vavilovites turgidus* zone; Dagys and Ermakova 1996).

Other than *Otoceras concavum* Tozer, *Otoceras gracile* Tozer has also been found from the upper Changhsingian *Otoceras concavum* zone in Arctic Canada (Tozer 1994) and South Verkhoyansk (this study). The earliest Induan *Otoceras boreale* Spath is known from four regions of the Boreal Superrealm: Arctic Canada (Tozer 1994), South Verkhoyansk (Zakharov 1971, 1978, 2002; Arkhipov 1974; Dagys and Ermakova 1996; this study), Svalbard (Petrenko 1963; Korchinskaya 1982; Nakazawa et al. 1987) and Greenland (Spath 1930, 1935).

Among the possible earliest representatives of the genus *Otoceras* from southern higher palaeolatitudes *Otoceras?* sp. may be apparently mentioned. It was recently found in the P–T boundary beds in Western Australia (northern Perth Basin, Redback-2 core; G. Shi unpublished data). The revision of *Otoceras* from the Himalayan province (Chao et al. 2017) shows that a single species of this genus is known there. According to Chao et al. (2017), *Otoceras undatum* (Griesbach), *O. fissisellatum* Diener, *O. parbati* Diener, *O. clivei* Diener, *O. draupadi* Diener, *O. dieneri* Spath and *O. latilobatum* Wang from the Himalayan province are younger synonyms of the *Otoceras woodwardi* Griesbach. If this is true, only a single *Otoceras woodwardi (=Otoceras latisellatum)* zone can be recognised within *Otoceras*-bearing sequences in that region. This corresponds to the *Otoceras boreale* zone of the Boreal Superrealm.

Ceratitid ammonoids of the suborder Otoceratina (Shevyrev and Ermakova (1979)) are represented by the single superfamily Otoceratoidea (Hyatt (1900)) and the three families: (1) the Wuchiapingian Anderssonoceratidae (Ruzhencev (1959)) (*Anderssonoceras*, *Lenticoceltites* and *Pericarinoceras*; Bogoslovskaya et al. 1999); (2) the Wuchiapingian–Changhsingian Araxoceratidae (Ruzhencev (1959)) (*Araxoceras*, *Eoaraxoceras*, *Rotaraxoceras*, *Prototoceras*, *Discotoceras*, *Urartoceras*, *Pseudotoceras*, *Vescotoceras*, *Dzhulfoceras*, *Vedioceras*, *Avushoceras*, *Periptychoceras*, *Anfuceras*, *Kingoceras*, *Abadehceras*, *Julfotoceras*, *Konglingites*, *Jinjiangoceras*, *Kiangsiceras* and *Sanyangites*; Zhou et al. 1999; Bogoslovskaya et al. 1999); and (3) the Changhsingian–Induan Otoceratidae (Hyatt (1900)) (*Anotoceras*, *Otoceras* and *Metotoceras*; Shevyrev 1968).

The suture lines of adult individuals of all Boreal species of the genus *Otoceras* are characterised by the presence of a tie-in at the top of the third lateral saddle, which was apparently inherited directly from Permian ammonoids, some of which (e.g. *Avushoceras*; Zakharov and Pavlov 1986) carry this feature on the third saddle of their suture line.

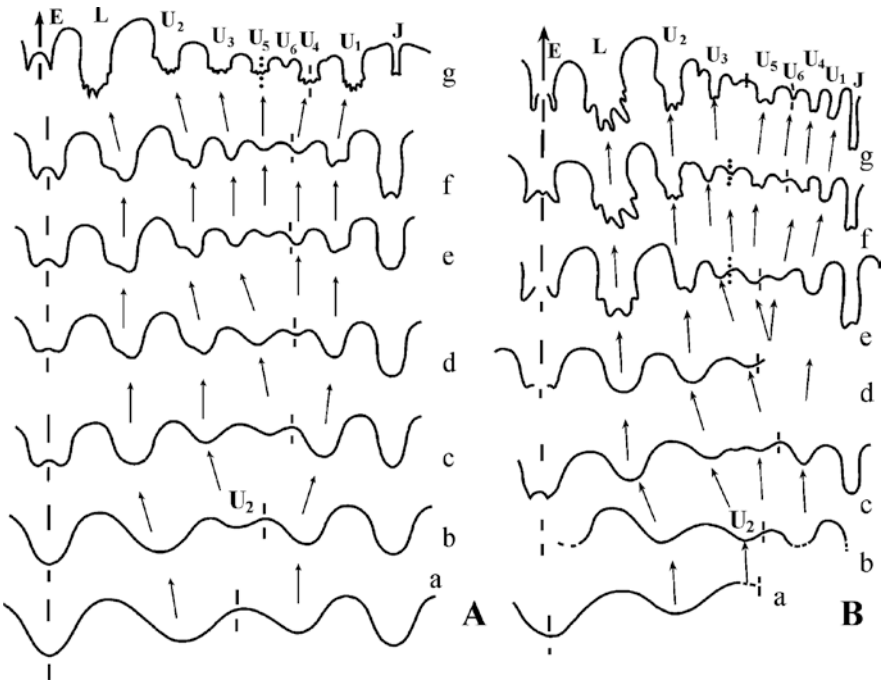

Fig. 10.11 Onthogenetic development of *Otoceras* from the Tethys and the Boreal Superrealm: (**a**) *O. woodwardi* Griesbach suture lines (Schindewolf 1968), with indication of Wedekind's (1916) lobe indexes; (**b**) *O. boreale* Spath suture lines (with indication of Wedekind's (1916) lobe indexes), based on samples 50/803 (stages a–c) and 33/803 (stages e–g) from the Nikolkin Klyuch section (a) at $W = 0.72$ mm; (b) at $H = 1.04$ mm and $W = 1.43$ mm; (c) at $H = 1.25$ mm and $W = 2.1$ mm; (d) at $H = 1.43$ mm and $W = 2.65$ mm; (e) at $H = 2.8$ mm and $W = 4.2$ mm; (f) at $H = 6.2$ mm and $W = 9.5$ mm; (g) at $H = 20.0$ mm and $W = 26.0$ mm

The similarity of onthogenetic development of suture lines in *Otoceras woodwardi* (Schindewolf 1968) and *O. boreale* (Fig. 10.11) which are common in Southern and Northern palaeohemispheres, respectively, gives some grounds for a monophyletic origin of the genus *Otoceras*.

Bando (1973) considered that the late Permian araxoceratid *Avushoceras jakowlevi* Ruzhencev was most intimately related to *Otoceras concavum* Tozer. Our data on the great similarity of suture lines of *Avushoceras jakowlevi* Ruzhencev from the Wuchiapingian–Changhsingian boundary transition in Transcaucasia and representatives of *Otoceras* from the uppermost Changhsingian and lowermost Induan in the Verkhoyansk area (Fig. 10.12) are in agreement with Bando's (1973) suggestion. Furthermore, juvenile *Otoceras* shells closely resemble the adult *Avushoceras* (Zakharov 1978, plate 3), reflecting possible anabolic development in the phylogenetic lineage *Avushoceras–Otoceras*. However, additional data is required to confirm this theory, which should take into account that the inner shell structure for representatives of the suborder Otoceratina is known only from *Otoceras*. The latter is characterised by a very primitive inner shell structure

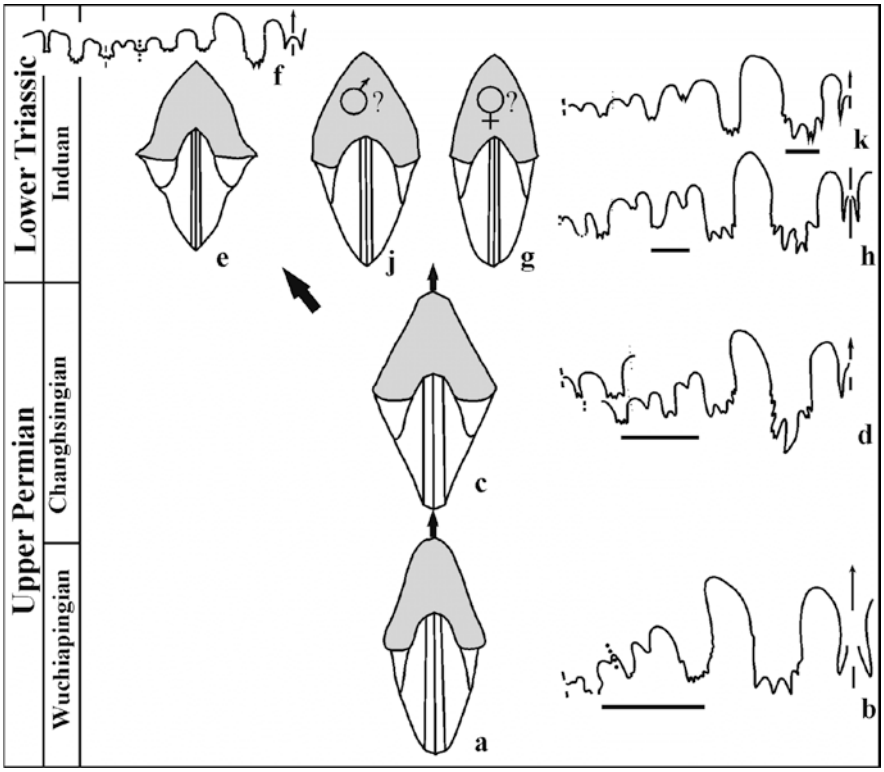

Fig. 10.12 Hypothetical evolutional trend of the Otoceratoidea. (a, b) *Avushoceras jakovlevi* Ruzhencev; (c, d) *Otoceras concavum* Tozer; (e, f) *O. woodwardi* Griesbach; (g, h) *O. boreale* Spath (morpha A); (j, k) *O. boreale* Spath (morpha B)

including retrochoanitic septal necks in both early and late ontogenetic stages and ventral position of the siphuncle in early ontogenetic stages (Zakharov 1978, Plate 3).

Late Permian Otoceratoidea (Araxoceratidae and Anderssonoceratidae) are known only from equatorial and neighbouring palaeoregions, such as South China (Zhao et al. 1978), Iran (Bando 1973; Zakharov et al. 2010), Transcaucasia (e.g. Kotlyar et al. 1983) and Mexico (Spinosa et al. 1970). However, representatives of the genus *Otoceras* are characterised by their bipolar distribution (Zakharov et al. 2008): in the Boreal Superrealm, Himalayan province of the Tethys (and possibly Gondwana Superrealm) (Fig. 10.13). We associate the migration of ancestral forms of *Otoceras* and some associated ammonoid genera to higher palaeolatitude areas mainly with climatical changes at the very end of the Permian as inferred from O- and N-isotope data. As shown above, the coolest conditions for the Late Permian occurred during the middle Changhsingian. A subsequent gradual increase in temperature in the late Changhsingian, as suggested by N-isotopic evidence (this study) and by O-isotope thermometry data (the palaeotemperature of the habitat of conodonts in the North-

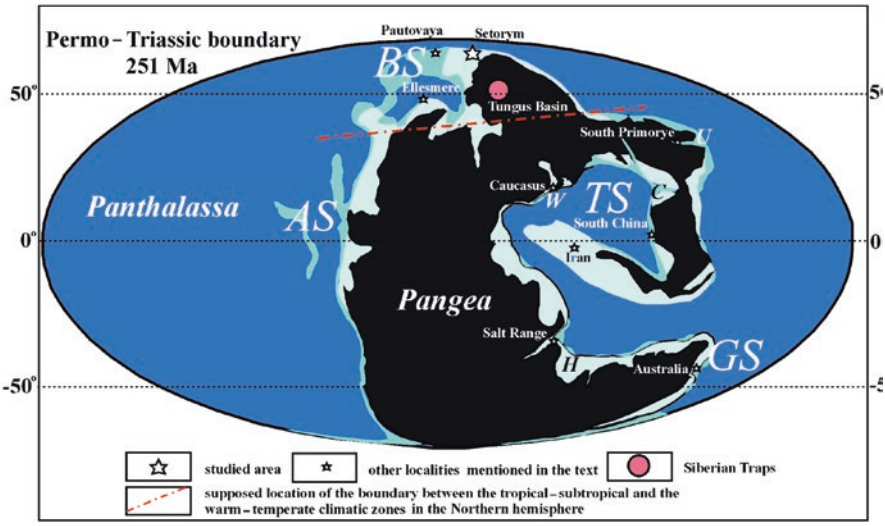

Fig. 10.13 Simplified palaeogeographical map of the Permian–Triassic boundary interval showing the relative location of the studied locality (Pravyi Suol, Setorym River basin) and other localities mentioned in the text (modified from Scotese 2014). Superrealms: *BS* Boreal. *TS* Tethyan. *AS* American, *GS* Gondwanan (Zakharov et al. 2008). Provinces: *C* Cathasian, *U* Ussurian, *W* Western-Tethyan (Zakharov et al. 2008)

Western Iran during the late Changhsingian reached ~38 °C; Schobben et al. 2014), caused the migration of ancestral forms of the genera *Otoceras*, *Tompophiceras* and others from the Iran–Transcaucasia area to cooler settings in the Boreal Superrealm. The general absence of *Otoceras* in the lowest Induan of the palaeoequatorial and palaeosubequatorial areas (South China, Transcaucasia and Iran) farther supports this proposed migration. Some groups of goniatitid, prolecanitid and ceratitid ammonoids that did not have any ability to migrate to higher (cooler) palaeolatitude areas became extinct presumably due to the extremely warm and possibly anoxic conditions that were most pronounced in equatorial and near-equatorial regions. This is consistent with the observation that almost all the known ammonoid survivors of the end-Permian mass extinction did so only within the Boreal Superrealm. In light of this, the Boreal Superrealm can be considered as a key refugium for the survival of otoceratid and some other ammonoids through the end-Permian mass extinction.

10.5 Conclusions

1. The ammonoid assemblages of the upper Changhsingian *Otoceras concavum* zone in the South Verkhoyansk region, as in Arctic Canada, are represented by two species belonging to the family Otoceratidae: *Otoceras concavum* Tozer and *Otoceras gracile* Tozer. The first representatives of *Tompophiceras* (Dzhulfitidae)

as well as *Episageceras* (Sageceratidae) in the South Verkhoyansk region have been found in the lowest division of the Indian (*Otoceras boreale* zone).

2. The absence of very low $\delta^{15}N_{sed}$ values (below −0.9‰ values that are commonly seen in the middle and low palaeolatitude areas) in Permian and Triassic strata of the Boreal Superrealm suggests accumulation under a relatively cooler climatic regime. However, the global trend towards warming across the P–T boundary transition is also seen in the Boreal regions.
3. According to biostratigraphical and palaeogeographical data, almost all the known ammonoid phylogenetic lineages that survived the mass extinction at the end of the Permian were able to accomplish this survival of only within the Boreal Superrealm. This suggests that the region was a key refugium for the survival of at least some otoceratid and dzhulfitid ammonoids during the development of lethally hot temperatures and possibly anoxic conditions in the Tethys. Since there is no evidence for Permian–Triassic glaciation in the Boreal region it seems likely that the conditions in this region were more favourable for the development of ammonoids even during the period of the end-Permian mass extinction, which was most pronounced in the Tethys.
4. A comparative morphological analysis of the species belonging to the genus *Otoceras*, which has bipolar geographic distribution, leads us to assume its monophyletic origin from araxoceratid *Avushoceras*, known from the Wuchiapingian–Changhsingian boundary transition in Transcaucasia.

Acknowledgements N-isotope analyses by E. Riegler (BLT Wiselbburg Research Center HBLFA Francisco-Josephinum, Austria) are gratefully acknowledged. We are also grateful to I.V. Brynko, I.V. Budnikov, S.S. Burnatyj, I.L Vedernikov, A.N. Kilyasov, V.I. Makoshin, A.N. Naumov and A.M. Popov from Magadan, Vladivostok and Yakutsk for their organising and taking part in our expeditions in the South Verkhoyansk region. Our special thanks to Tretyakovs, Felix F. and Maxim F., for the opportunity to use the Yakutsk Federal University field base on the left bank of the Vostochnaya Khandyga River (the Tompo Training Ground). This research was funded by the grants RFBR no. 18-05-00023, 18-05-00191, and 20-05-00604, in part by the Program for Improvement of the Competitiveness of Kazan (Volga River) Federal University among the world's leading research and educational centers, and also in part (monographic study of new invertebrate collections from the South Verkhoyansk region) by the Russian Scientific Foundation, grant no. 19-17-00178. A monographic study of P-T cephalopods is done on state assignments for a number institutions of the Russian Academy of sciences (FEGI, DPMGI, and IPGG). D.P.G. Bond acknowledges funding from the Natural Environment Research Council (Grant NE/JO1799X/1) and the Royal Society (International Exchanges scheme-project "Volcanic and climatic impacts on Permian biota across Russian ecological zones").

References

Algeo TJ, Rowe H, Hower JC, Schwark L, Hermann A, Heckel PH (2008) Oceanic denitrification during Late Carboniferous glacial-interglacial cycles. Nat Geosci 1:709–714

Algeo T, Henderson CM, Ellwood B, Rowe H, Elswick E, Bates S, Lyons T, Hower JC, Smith C, Maynard B, Nays LE, Summons RE, Fulton J, Freeman KN (2012) Evidence for a

diachronous Late Permian marine crisis from Canadian Arctic region. Geol Soc Am Bull 124(9/10):1424–1448
Algeo TJ, Meyers PA, Robinson RS, Rowe H, Jiang GQ (2014) Icehouse-greenhouse variations in marine denitrification. Biogeosciences 11:1273–1295
Altabet MA, Francois R, Murray DW, Ptell WL (1995) Climate-related variations in denitrification in the Arabian Sea from sediment $^{15}N/^{14}N$ ratios. Nature 373:506–509
Arkhipov YV (1974) Stratigrafiya triasaovykh otlozhenij vostochnoj Yakutii (Triassic stratigraphy of Eastern Yakutia). Yakutskoye knizhnoye izdatelstvo, Yakutsk, 273 p (in Russian)
Bando Y (1973) On the Otoceratidae and Ophiceratidae. Sci Rep Tohoku Univ 6:337–351
Baud AM, Margaritz M, Holser WT (1989) Permian–Triassic of the Tethys: carbon isotope stratigraphy. Geol Rundsch 78:649–677
Bauersachs T, Schouten S, Compaore J, Wollenzien U, Stal LJ, Damsté JSS (2009) Nitrogen isotopic fractionation associated with growth on dinitrogen gas and nitrate by cyanobacteria. Limnol Oceanogr 54(4):1403–1411
Biakov AS, Vedernikov IL (2007) Evidence for anoxia in deep environments of Northeast Asia. Dokl Earth Sci 417A(9):1325–1327
Biakov AS, Zakharov YD, Horacek M, Richoz S, Kutygin RV, Ivanov YY, Kolesov EV, Konstantinov AG, Tuchkova MI, Mikhalitsyna TI (2016) New data on the structure and age of the terminal Permian strata in the South Verkhoyansk region (northeastern Asia). Russ Geol Geophys 57:282–293
Biakov AS, Kutygin RV, Goryachev NA, Burnatny SS, Naumov AN, Yadrenkin AV, Vedernikov IL, Tretyakov AV, Brynko IV (2018) Discovery of the late Changhsingian bivalve complex and two fauna extinction episodes in northeastern Asia at the end of the Permian. Dokl Biol Sci 480:78–81
Bjerager M, Seidler L, Stemmerik L, Surlyk F (2006) Ammonoid stratigraphy and sedimentary evolution across the Permian–Triassic boundary in East Greenland. Geol Mag 143(5):635–656
Bogoslovskaya MF, Kuzina LF, Leonova TB (1999) Classification and distribution of Late Palaeozoic ammonoids. In: Rozanov AY, Shevyrev AA (eds) Iskopaemye tsefalopody noveishiye dostizhenuya v ikh izuchenii (Fossil cephalopods: recent advances in their study). PIN RAN, Moscow, pp 89–124, (in Russian)
Bond DG, Wignall PB (2010) Pyrite framboid study of marine Permian–Triassic boundary sections: a complex anoxic event and its relationship to contemporaneous mass extinction. Geol Soc Am Bull 122(7/8):1265–1279
Boulila S, Laskar J, Haq BU, Galbrun B, Hara N (2018) Long-term cyclicities in Phanerozoic sea-level sedimentary record and their potential drivers. Supplementary material (SM1 & SM2). https://arxiv.org/pdf/1803.05623
Brosse M, Bucher H, Goudemand N (2016) Quantitative biochronology of the Permian-Triassic boundary in South China based on conodont unitary associations. Earth Sci Rev 155:153–171
Burgess SD, Bowring S, Shen S (2014) High-precision timeline for Earth's most severe extinction. Proc Natl Acad Sci 111(9):3316–3321
Chao Z, Bucher H, Shen S-Z (2017) Griesbachian and Dienerian (Early Triassic) ammonoids from Qubu in the Mt. Everest area, southern Tibet. Palaeoword 26:650–662
Cockell CS, Cathing DC, Davis WL, Snook K, Kepner RL, Lee P, McKay CP (2000) The ultraviolet environment of Mars: biological implications past, present and feature. Icarus 146(2):343–359
Dagys A, Ermakova S (1996) Induan (Triassic) ammonoids from north-eastern Asia. Rev Paléobiol 15(2):401–447
Dagys AS, Arkhipov YV, Bytchkov YM (1979) Stratigrafiya triasovoj sistemy Severo-Vostoka Azii (Triassic stratigraphy of north-eastern Asia). Nauka, Moscow, 244 p (in Russian)
Dagys AS, Arkhipov YV, Truschelyev AM (1984) Excursion 054. Permian and Triassic deposits in Yakutiya. Svodnyj putevoditel ekskursij 052, 053, 054. 055 (27 Mezhdunarodnyi Geologicheskij Kongress) Yakutskaya ASSR, Sibirskaya Platforma (Summary Field Guide Book of excursions 052, 053, 05 and 055 (27th International Geological Congress)). Nauka, Novosibirsk, p 68–89. (in Russian)

Dagys AS, Dagis AA, Kazakov AM, Konstantinov AG, Kurushin NI (1986) Lower Induan biostratigraphy of eastern Verkhoyansk. In: Yanshin AL, Dagys AS (eds) Biostratigrafiya mezozoya Sibiri i Dalnrgo Vostoka (Mesozoic biostratigraphy of Siberia and Far East). Nauka, Novosibirsk, pp 21–31, (in Russian)

Diener C (1897) The Cephalopoda of the Lower Trias. Palaeontologica Indica 15(2/1):1–181

Domokhotov SV (1960) Induan stage and *Otoceras* zone of the eastern Verkhoyansk area. In: Kobelyatskij IA (ed) Materialy po geologg i poleznym iskopaemym Yakutskoj ASSR. 1 (Materials on geology and minerals of the Yakut ASSR. 1). Yakutskoye knizhnoye izdatelstvo, Yakutsk, pp 111–120, (in Russian)

Dustira AM, Wignall PB, Joachimski M, Blomeier D, Hartkopf-Fröder C, Bond DPG (2013) Gradual onset of anoxia across the Permian–Triassic boundary in Svalbard, Norway. Palaeogeogr Palaeoclimatol Palaeoecol 374:303–313

Garbelli C, Angiolini L, Brand U, Shen S, Jadoul F, Azmy K, Posenato R, Cao C (2014) The paradox of the Permian global oceanic anoxia. Permophiles 61:26–28

Goudemand N, Romano C, Brayard A, Hochuli PA, Bucher H (2013) Comment on "Lethally hot temperatures during the Early Triassic greenhouse". Science 339:1033a–1033c

Grasby SE, Beauchamp B (2008) Intrabasin variability of the carbon-isotope record across the Permian–Triassic transition, Sverdrup Basin, Arctic Canada. Chem Geol 253:141–150

Grasby SE, Sanei H, Beachamp B, Chen Z (2013) Mercury deposition through the Permo-Triassic biotic crisis. Chem Geol 351:209–216

Grasby SE, Beauchamp B, Bond DPG, Wignall P, Talavera C, Galloway JM, Piepjohn K, Reinhardt L, Blomeier D (2015) Progressive environmental deterioration in northwestern Pangea leading to the latest Permian extinction. Geol Soc Am Bull 127:1331–1347

Grasby SE, Beauchamp B, Knies J (2016) Early Triassic productivity crises delayed recovery from world's worst mass extinction. Geology 44:779. https://doi.org/10.1130/G38141.1

Grasby SE, Beauchamp B, Bond DPG, Wignall P, Sanei H (2018) Mercury anomalies associated with three extinction events (Capitanian crises, latest Permian extinction and the Smithian/Spathian extinction in NW Pangea). Geol Mag 153:285–297

Grigoryan AG, Alekseev AS, Joachimski MM, Gatovsky YA (2015) Permian–Triassic biotic crisis: a multidisciplinary study of Armenian sections. In: Nurgaliev DK (ed) XVIII International Congress on the Carboniferous and Permian (August 11–15, 2015, Kazan, Russia), Kazan, Kazan University Press, abstract volume (p 74)

Hammer D, Jones MT, Schneebeli-Hermann E, Hansen BB, Bucher H (2019) Are Early Triassic extinction events associate with mercury anomalies? A reassessment of the Smithian/Spathian boundary extinction. Earth Sci Rev 195:179. https://doi.org/10.1016/j.earscirev.2019.04.016

Hermann E, Hochuli PA, Bucher H, Vigran JO, Wessert H, Bernasconi SM (2010) A close-up view of the Permian-Triassic boundary based on expanded organic carbon isotope records from Norway (Trøndelag and Finnmark platform). Global Planet Change 74:156–167

Hermann E, Hochuli PA, Méhay S, Bucher H, Brühwiler T, Ware D, Hautmann M, Roohi G, ur-Rehman K, Yaseen A (2011) Organic matter and palaeoenvironmental signals during the early Triassic biotic recovery: the salt range and Surghar range records. Sediment Geol 234:19–41

Hochuli PA, Vigran JO, Hermann E, Bucher H (2010) Multiple climatic changes around the Permian–Triassic boundary event revealed by an expanded palynological record from mid-Norway. GSA Bull 122(5/6):884–896

Horacek M, Brander R, Abart R (2007a) Carbon isotope record of the P/T boundary and the Lower Triassic in the Southern Alps: evidence for rapid changes in storage of organic carbon. Palaeogeogr Palaeoclimatol Palaeoecol 252:347–354

Horacek M, Richoz S, Brandner R, Krystyn L, Spötl C (2007b) Evidence for recurrent changes in Lower Triassic oceanic circulation if the Tethys: the Delta ^{13}C record from marine sections in Iran. Palaeogeogr Palaleoclimatol Palaeoecol 252:355–369

Horacek M, Wang X-D, Grossman EL, Richoz S, Cao Z (2007c) The carbon-isotope curve from the Chaohu section, China: different trends at the Induan-Olenekian boundary or diagenesis? Albertiana 35:41–45

Horacek M, Koike T, Richoz S (2009) Lower Triassic $\delta^{13}C$ isotope curve from shallow-marine carbonates in Japan, Panthalassa realm: confirmation of the Tethys $\delta^{13}C$ curve. J Asian Earth Sci 3(6):481–490. https://doi.org/10.1016/j.jseaes.2008.05.005

Horacek M, Brandner R, Richoz R, Povoden E (2010) Lower Triassic sulphur isotope curve of marine sulphates from the Dolomites, N-Italy. Palaeogeogr Palaeoclimatol Palaeoecol 290(1–4):65–70. https://doi.org/10.1016/j.palaeo.2010.02.016

Hyatt A (1900) Ammonoidea. In: Zittel KA (ed) Textbook of palaeontology. C.R. Eastman, London, pp 502–592, 1st English ed

Isozaki Y (1997) Permo-Triassic boundary superanoxia and stratified superocean: records from lost deep sea. Science 276:235–238

Jenkyns HC, Gröcke DR, Hesselbo SP (2001) Nitrogen isotope evidence for mass denitrification during the early Toarcian (Jurassic) oceanic anoxic event. Paleoceanography 16:593–603

Jia C, Huang J, Kershaw S, Luo G (2012) Microbial response to limited nutrients in shallow water immediately after the end-Permian mass extinction. Geobiology 10:60–71

Joachimsky MM, Lai X, Shen S, Jiang H, Luo G, Chen B, Chen J, Sun Y (2012) Climate warming in the latest Permian and the Permian-Triassic mass extinction. Geology 40:195–198

Joachimski MM, Alekseev AS, Grigoryan A, Gatovsky YA (2020) Siberian Trap volcanism, global warming and the Permian-Triassic mass extinction: New insights from Armenian Permian-Triassic sections. The Geological Society of America Bulletin 132: 427–443. https://doi.org/10.1130/B35108.1

Kaiho K, Kajiwara Y, Nakano Y, Miura Y, Chen ZQ, Shi GR (2001) End-Permian catastrophe by a bolide impact: evidence of a gigantic release of sulfur from the mantle. Geology 29:815–818

Kaiho K, Chen ZQ, Sawda K (2009) Possible causes for a negative shift in the stable carbon isotope ratio before, during and after the end-Permian mass extinction in Meishan, South China. Aust J Earth Sci 56:799–808

Kato Y, Nakao K, Isozaki Y (2002) Geochemistry of Late Permian to Early Triassic pelagic cherts from southwest Japan: implications for an oceanic redox change. Chem Geol 182:15–34

Knies J, Grasby SE, Beuchamp B, Schubert CJ (2013) Water mass denitrification during the latest Permian extinction in the Sverdrup Basin, Arctic Canada. Geology 41(2):167–170

Knoll AH, Bambach RK, Payne JL, Pruss S, Fischer WW (2007) Palaeophysiology and end-Permian mass extinction. Earth Planet Sci Lett 256:295–313

Korchinskaya MV (1982) Obyasnitelnaya zapiska k stratngraficheskoj scheme mezozoya (triasa) Svalbarda (Explanatory note on the biostratigraphic scheme of the Mesozoic (Trias) of Spitsbergen). Sevmorgeologiya, Leningrad, 99 p (in Russian)

Korostelev VI (1972) Stratigrafia triasovykh otlozhenij Vostochnogo Verkhoyanya (Triassic stratigraphy of the Eastern Verkhoyansk area). Yakutskoye knizhnoye izdatelstvo, Yakutsk, 174 p (in Russian)

Korte C, Kozur HW (2010) Carbon-isotope stratigraphy across the Permian-Triassic boundary: A review. J Asian Earth Sci 39:215–235

Kotlyar GV, Zakharov YD, Koczyrkevicz BV, Kropacheva GS, Rostovcev KO, Chedija IO, Vuks GP, Guseva EA (1983) Pozdnepermskij etap evolyutsii organicheskogo mira (Dzhulfinskij i Dorashamskij yarusy SSSR) (Evolution of the latest Permian biota (Dzhulfian and Dorashamian regional stages in the USSR)). Nauka, Leningrad, 199 p (in Russian)

Kozur HW (2007) Biostratigraphy and event stratigraphy in Iran around the Permian-Triassic boundary (PTB): implications for the causes of the PTB biotic crisis. Global Planet Change 55:155–176

Kozur HW, Weems RE (2011) Detailed correlation and age of continental late Changhsingian and earliest Triassic beds: implications for the role of the Siberian trap in the Permian–Triassic biotic crisis. Palaeogeogr Palaeoclimatol Palaeoecol 308:22–40

Krull ES, Retallack GJ, Campbrll HJ, Lyon GL (2000) $\delta^{13}C_{org}$ chemostratigraphy of the Permian–Triassic boundary in the Maitai Group, New Zealand: evidence for high-latitudinal methane release. N Z J Geol Geophys 43:21–32

Kurushin NI (1987) Drevnejshie triasovye dvustvorchatye mollyuski Yakutii (The oldest Triassic bivalves from Yakutiya). In: Dagys AS (ed) Boreal'nyj trias (Boreal Triassic). Nauka, Moscow, pp 99–110, (in Russian)

Lozovsky VR (2013) Permian-Triassic crisis and its possible reason. Byulyuten Moskovskogo Obschestva Ispytatelej Prirody. Otdeleniye Geologicheskoye 88(1):49–58. (in Russian)

Luo G, Wang Y, Kump LR, Algeo TJ, Yang H, Xie S (2011) Enhanced nitrogen fixation in the immediate aftermath of the latest Permian marine mass extinction. Geology 39(7):647–650

Nakazawa K, Nakamura K, Kimura G (1987) Discovery of *Otoceras boreale* Spath from West Spitsbergen. Proc Japan Acad Ser B 63(6):171–174

Nakrem HA, Orchard M, Weitschart W, Hounslow MW, Beaity TW, Mørk A (2008) Triassic conodonts from Svalbard and the Boreal correlations. Polar Res 27(3):523–537

Noetling F (1904) Ueber *Medlicottia* Waag. und *Episageceras* n. g. aus den permischen und triadischen Schichten indiens. Neues Jahrbuch für Mineralogy, Geologie und Paläontologie 19:334–376

Parfenov LM, Kuzmin MI (2001) Tectonics, geodynamics and metallogeny of the Sakha Republic (Yakutia). MAIK Nauka Interperiodica, Moscow, 571 p

Petrenko VM (1963) Some important finds of Early Triassic fauna on Spitsbergen. Uchyonye Zapiski NIIGA 3:50–54. (in Russian)

Popow YN (1956) *Otoceras* in the lower Triassic of eastern Verkhoyansk. In: Kobelyatsky IA (ed) Materialy po geologii i poleznym iskopaemym Severo-Vostoka SSSR, vol 10. Magadan, Magadanskoye Knizhnoye Izdatelstvo, pp 64–81. (in Russian)

Popow YN (1958) Find of *Otoceras* in the lower Triassic of eastern Verkhoyansk. Izvestiya Akademii Nauk SSSR Ser Geol 12:105–109. (in Russian)

Popow YN (1961) Triasovye ammonoidei Severo-Vostoka SSSR (Triassic ammonoids of the North-Eastern USSR). Tudy NIIGA 79:1–180. (in Russian)

Robinson RS, Kienast M, Albuquerque AL, Altalet M, Contreras S, Holz R, Dubots N, Francois R, Galbraith E, Hsu T, Ivanochko T, Jaccard S, Kao S, Kiefer T, Kienast S, Lehmann M, Martinez P, McCarthy M, Möbius J, Pederson T, Quan TM, Ryabenko E, Schmittner A, Schneider R, Schneider-Mor A, Thunell R, Yang J (2012) A review of nitrogen isotope alteration in marine sediments. Paleoceanography 27:1–13

Romano C, Goudemand N, Vennemann TW, Ware D, Schneebeli-Hermann E, Hochuli PA, Brühwiler T, Brinkmann W, Bucher H (2013) Climatic and biotic upheavals following the end-Permian mass extinction. Nat Geosci 6:57–60

Ruzhencev VE (1959) Classification of the superfamily Otoceratacеae. Paleontologocheskij Zhurnal 2:57–67. (in Russian)

Sadovnikov GN (2008) On the position of the "point of the lower Triassic boundary in global stratotype". Stratigrafiya Geologicheskaya Correlyatsiya 16(1):34–50

Sadovnikov GN (2016) Evolution of the biome of the trap plateau of Central Siberia. Paleontologicheskij Zhurnal 5:87–99. (in Russian)

Saitoh M, Ueno Y, Nishizawa M, Isozaki Y, Takai K, Yao J, Ji Z (2014) Nitrogen isotope chemostratigraphy across the Permian-Triassic boundary at Chaotian, Sichuan, South China. J Asian Earth Sci 93:113–128

Schindewolf OH (1968) Studien zur Stammesges chichte der Ammoniten, Lieferung 7. Abhandlungen der mathematisch-naturwissenschaftlichen Klasse. Akademie der Wissenschaften und der Literatur in Mainz 3:1–171

Schobben M, Joachimski MM, Korn D, Leda L, Korte C (2014) Palaeotethys seawater temperature rise and an intensified hydrological cycle following the end-Permian mass extinction. Gondw Res 26:675–683

Scotese CR (2014) Atlas of Permo–Triassic paleogeographic maps (Mollweide projection), maps 43—52, Volumes 3 & 4 of the PALEOMAP Atlas for ArcGIS, PALEOMAP Project, Evanston, IL. doi: https://doi.org/10.13140/2.1.2609.9209

Shevyrev AA (1968) Triassic ammonoids of the South USSR. Trudy PIN 110:1–272. (in Russian)

Shevyrev AA, Ermakova SP (1979) Systematics of ceratites. Paleontologicheskij Zhurnal 1:52–58. (in Russian)

Sobolev ES (1989) Triasovye nautilidy Severo-Vostochnoy Azii (Triassic nautilids of northeastern Asia). Nauka, Siberian Branch, Novosibirsk, 192 p (in Russian)
Song H, Tong J, Algeo TJ, Horacek M, Qiu H, Tian L, Chen Z-Q (2013) Large vertical $\delta^{12}C_{DIC}$ gradients in Early Triassic seas of the South China craton: implications for oceanographic changes related to Siberian Traps volcanism. Global Planet Change 105:7–20
Spath LF (1930) The Eo-Triassic invertebrate fauna of East Greenland. Medd Grønland 83(1):1–90
Spath LF (1935) Additions to the Eo-Triassic invertebrate fauna of East Greenland. Medd Grønland 98(2):1–115
Spinosa C, Furnish WM, Glenister BF (1970) Araxoceratidae, Upper Permian ammonoids, from the Western Hemisphere. J Paleo 44(4):730–736
Sun Y, Joachimski MM, Wignall PB, Yan C, Chen Y, Jiang H, Wang L, Lai X (2012) Lethally hot temperatures during the Early Triassic Greenhouse. Science 338:366–370
Takashi S, Kaiho K, Oba M, Kakegawa T (2010) A smooth negative shift of organic carbon isotope ratios at an end-Permian mass extinction horizon in central pelagic Panthalassa. Palaeogeogr Palaeoclimatol Palaeoecol 292:532–539
Takashi S, Kaiho K, Kori RS, Hori RS, Gorjan P, Watanabe T, Yamakita S, Aita Y, Takemura A, Spörli KB, Kakegawa T, Oba M (2013) Sulfur isotope profiles in the pelagic Panthalassic deep sea during the Permian-Triassic transition. Global Planet Change 105:68. https://doi.org/10.1016/J.gloplacha.2012.12.006
Tozer ET (1994) Canadian Triassic ammonoid faunas. Geol Surv Can Bull 467:1–663
Twitchet RJ, Looy CV, Morant ER, Vissehes H, Wignall PB (2001) Rapid and synchronous collapse of marine and terrestrial ecosystems during the end-Permian biotic crisis. Geology 29(4):351–354
Wedekind R (1916) Über Lobus, Suturallobus und Inzision. Zentralblatt fü Geologie und Paläontologie 8:185–195
Wignall PB, Hallam A (1992) Anoxia as a cause of the Permian-Triassic mass extinction: facies evidence from northern Italy and the western United States. Palaeogeogr Palaeoclimatol Palaeoecol 102:215–237
Wignall PB, Twitchet RJ (1996) Oceanic anoxia and the end-Permian mass extinction. Science 272:1155–1158
Wignall PB, Twitchet RJ (2002) Extent, duration, and nature of the Permian-Triassic superanoxic event. Geol Soc Am Spec Paper 356:395–413
Wignall PB, Bond DPG, Sun Y, Grasby SE, Beauchamp B, Joachimski MM, Blomeier DPG (2015) Ultra-shallow-marine anoxia in an Early Triassic shallow-marine clastic ramp (Spitsbergen) and the suppression of benthic radiation. Geol Mag 153:316–331
Yin H, Song FK (2013) Mass extinction and Pangea integration during the Paleozoic-Mesozoic transition. Sci China Earth Sci 56(1):1–13
Yin H, Zhang K (1996) Eventostratigraphy of the Permian-Triassic boundary at Meishan section, South China. In: Yyn H (ed) The Palaeozoic-Mesozoic boundary (candidates of global stratotype section and point of the Permian–Triassic boundary). China University of Geosciences Press, Wuhan, pp 84–96
Yin H, Xie S, Luo G, Algeo T, Zhang K (2012) Two episodes of environmental change at the Permian–Triassic boundary of the GSSP section Meishan. Earth Sci Rev 115:162–172
Zakharov YD (1971) *Otoceras* of the boreal realm. Paleontologicheskij Zhurnal 3:50–59. (in Russian)
Zakharov YD (1978) Rannetriasovye ammonoidei vostoka SSSR (Early Triassic ammonoids of the east USSR). Nauka, Moscow, 224 p (in Russian)
Zakharov YD (1995) The Induan–Olenekian boundary in the Tethys and Boreal realm. Annali dei Musei Civici di Rovereto Sezione Archeologia, Storia e Scienze Naturali 11:133–156
Zakharov YD (2002) Ammonoid succession of Setorym River (Verkhoyansk area) and problem of Permian–Triassic boundary in Boreal realm. J China Univ Geosci 13(2):107–123
Zakharov YD (2003) Ammonoid succession in the Lower Triassic of the Verkhoyansk area and problem of the Otoceratacеae, Xenodiscaceae and Proptychitaceae phylogeny. In: Kryukov AP, Yakimenko LV (eds) Problemy evolyutsii (Problems of evolution), vol 5. Dalnauka, Vladivostok, pp 244–262. (in Russian)

Zakharov YD, Moussavi Abnavi N (2013) The ammonoid recovery after the end-Permian mass extinction: evidence from the Iran-Transcaucasia area, Siberia, Primorye and Kazakhstan. Acta Palaeontol Pol 58(1):127–147

Zakharov YD, Pavlov AM (1986) The first find of an araxoceratid ammonoid in the Permian of the eastern part of the USSR. In: Zakharov YD, Onoprienko YI (eds) Permo-triasovye sobytiya v razvitii organicheskogo mira severo-vostochnoj Asii (Permian-Triassic events during the biotic evolution of North-East Asia). Academy of Sciences of the USSR, Far-Eastern Scientific Centre, Vladivostok, pp 74–85. (in Russian)

Zakharov YD, Popov AM (2014) Recovery of brachiopod and ammonoid faunas following the end-Permian crisis: additional evidence from the lower Triassic of the Russian Far East and Kazakhstan. Aust J Earth Sci 25(1):1–44

Zakharov YD, Naidin DP, Teis RV (1975) Oxygen isotope composition Early Triassic cephalopod shells of Arctic Siberia and salinity of the Boreal basins at the beginning of the Mesozoic. Izvestiya Akademii Nauk SSSR Ser Geol 4:101–113. (in Russian)

Zakharov YD, Boriskina NG, Cherbadzhi AK, Popov AM, Kotlyar GV (1999) Main trends in Permo–Triassic shallow-water temperature changes: evidence from oxygen isotope and Ca-Mg ratio data. Albertiana 23:11–22

Zakharov YD, Biakov AS, Baud A, Kozur H (2005) Significance of Caucasian sections for working out carbon-isotope standard for Upper Permian and Lower Triassic (Induan) and their correlation with the Permian of north-eastern Russia. J China Univ Geosci 16(2):141–151

Zakharov YD, Popov AM, Biakov AS (2008) Late Permian to Middle Triassic palaeogeographic differentiation of key ammonoid groups: evidence from the former USS. Polar Res 27(3):441–468

Zakharov YD, Mousavi Abnavi N, Ghaedi M (2010) New species of Dzhulfian (Late Permian) ammonoids from the Hambast Formation of Central Iran. Paleontol J 44(6):614–631

Zakharov YD, Biakov AS, Horacek M (2014) Global correlation of basal Triassic layers in the light of the first carbon isotope data on the Permian–Triassic boundary in Northeast Asia. Russ J Pac Geol 8(1):3–19

Zakharov YD, Biakov AS, Richoz S, Horacek M (2015) Importance of carbon isotopic data of the Permian-Triassic boundary layers in the Verkhoyansk region for the global correlation of the basal Triassic layer. Dokl Earth Sci 460(1):1–5

Zakharov YD, Horacek M, Popov AM, Bondarenko LG (2018a) Nitrogen and carbon isotope data of Olenekian to Anisian deposits from Kamenushka/south Primorye, far-eastern Russia and their palaeoenvironmental significance. Aust J Earth Sci 29(4):837–853

Zakharov YD, Horacek M, Shigeta Y, Popov AM, Bondarenko LG (2018b) N and C isotopic composition of the lower Triassic of southern Primorye and reconstruction of the habitat conditions of marine organisms. Stratigr Geol Correl 26(5):534–551

Zakharov YD, Horacek M, Shigeta Y, Popov AM, Maekawa T (2018c) N- and C isotopic composition of the lower Triassic of south Primorye and reconstruction of habitat conditions of marine organisms after end Permian mass extinction at the end of the Permian. Dokl Earth Sci 478(2):161–165

Zakharov YD, Biakov AS, Horacek M, Goryachev NA, Vedernikov IL (2019) The first data on the N isotopic composition of the Permian and Triassic of northeastern Russia and their significance for paleotemperature reconstructions. Dokl Earth Sci 484(1):21–24

Zakharov YD, Horacek M, Biakov AS (in press) First data on N-isotope composition of the Permian-Triassic in the Verkhoyansk region and their significance for reconstruction of marine environments. Stratigrafiya. Geologicheskaya Korrelyatsiya (in Russian)

Zhao J, Liang X, Zheng Z (1978) Late Permian cephalopods of South China. Palaeontol Sin New Ser B 154(12):1–194

Zhou Z, Glenister BF, Furnish WM, Spinosa C (1999) Multi-episodal extinction and ecological and differentiation of Permian ammonoids. In: Rozanov AY, Shevyrev AA (eds) Fossil cephalopods: recent advances in their study. Paleontological Institute RAS, Moscow, pp 195–212